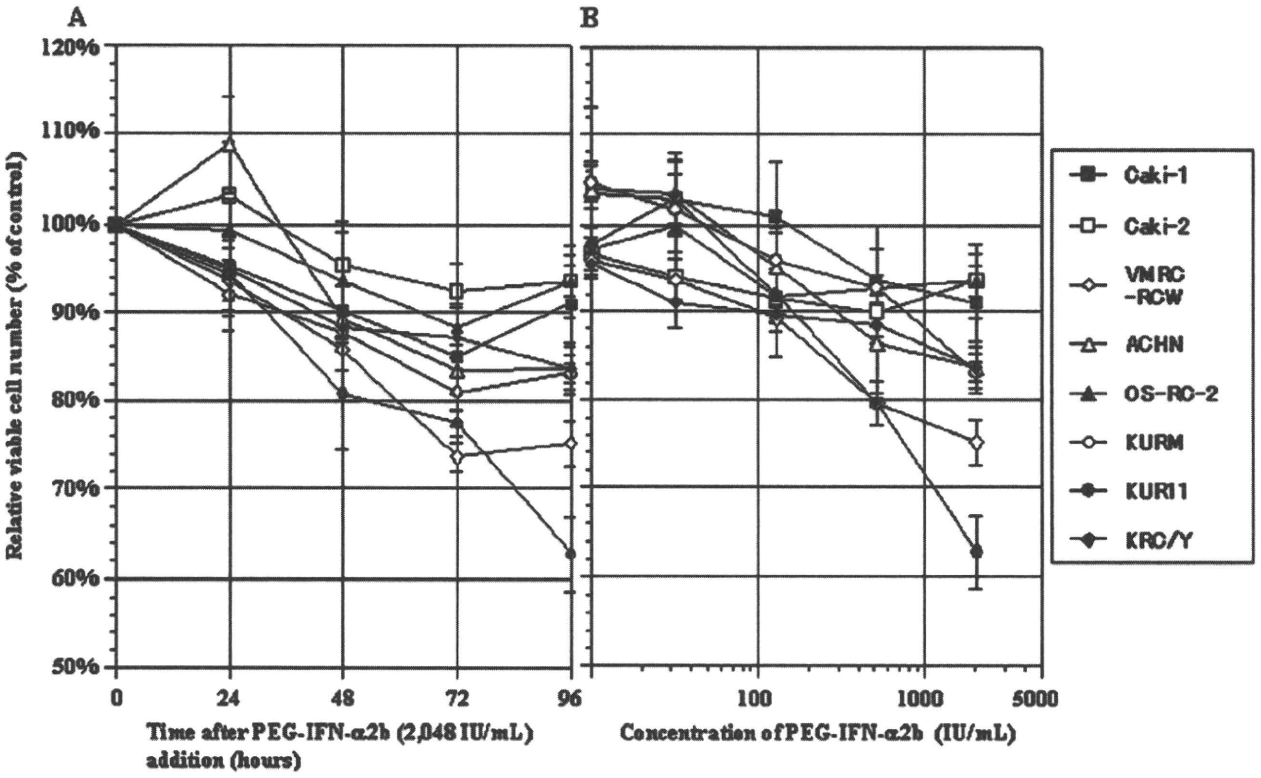

Figure 1. Anti-proliferative effects of PEG-IFN-α2b. (A) Chronological changes in relative viable cell number (% of the control) after adding 2,048 IU/ml of PEG-IFN-α2b. Growth was significantly suppressed over time in 2 cell lines (KUR11 and KRC/Y). (B) Ninety-six hours after adding 8, 32, 128, 512 or 2,048 IU/ml of PEG-IFN-α2b. Cell proliferation was suppressed in a dose-dependent manner in 6 cell lines (all but Caki-2 and OS-RC-2). Eight samples were used in each experiment. The experiment was repeated at least three times for each cell line. The values represent the average ± SE.

8 and 11). The clinical daily dose of IFN-α2b for human RCC is $600x10^4$ IU/body ($1.2x10^5$ IU/kg), and this is approximately four times the lowest dose ($3.2x10^4$ IU/kg) used in this experiment. Tumor size was measured in two directions by using calipers on the first and second days of s.c. injection (day 1 and 2) and then once every 2 days until day 14, and tumor volume (mm^3) was estimated by using the equation: Length x $(Width)^2$ x 0.5. Mouse body weight was measured on day 0, 8 and 14. On day 15, all mice were sacrificed and the tumors were removed.

The animals received human care according to criteria outlined in the 'Guide for the Care and Use of Laboratory Animals' prepared by the National Academy of Sciences and published by the National Institutes of Health (NIH publication 86-23, revised 1985).

Effects of combination therapy of PEG-IFN-α2b and 5-FU on RCC cell proliferation in nude mice. VMRC-RCW cells ($7.5x10^6$ cells/mouse) were subcutaneously injected into 4-week-old female BALB/c athymic nude mice (n=58). The mice were divided into 7 groups (n=8 or 9 each) on day 7 when tumor size reached ~10 mm in diameter, and each group was assigned to one of the 7 treatments: i) PEG-IFN-α2b alone (6,400 IU); ii) IFN-α2b alone (6,400 IU); iii) low dose 5-FU alone (160 μg); iv) high dose 5-FU alone (320 μg); v) combination therapy of PEG-IFN-α2b (6,400 IU) and low dose 5-FU; vi) combination therapy of IFN-α2b (6,400 IU) and low dose 5-FU; and (vii) control.

5-FU was administered intra-abdominally every day for 2 consecutive weeks. The dose of 5-FU (160 μg/mouse, 8 mg/kg) is comparable to the clinical dose.

Tumor size measurement and IFN administration were performed in the same manner as described above. On day 15, all mice were sacrificed and each tumor was removed. After the tumor weight was measured, half of the obtained tumors were used for histological examination and the other half were used for quantitative real-time RT-PCR.

The number of cells showing characteristics of apoptosis such as cytoplasmic shrinkage, chromatin condensation and nuclear fragmentation was counted in ten 0.25 mm^2 areas within an H&E-stained specimen, and the average number per area was obtained. The TUNEL technique (ApopTag® Peroxidase In Situ Apoptosis Detection Kits, Chemicon International, CA, USA) was also used to detect apoptotic cells. The average number of TUNEL-positive cells per area was obtained as described above.

Immunohistochemistry. Double immunohistochemical staining was performed by using anti-mouse endothelial cell (anti-CD34) antibody, anti-human α smooth muscle actin (α-SMA) antibody and histofine simple stain mouse Max-Po (Rat) kits (Nichirei, Tokyo, Japan) as described elsewhere (16). We

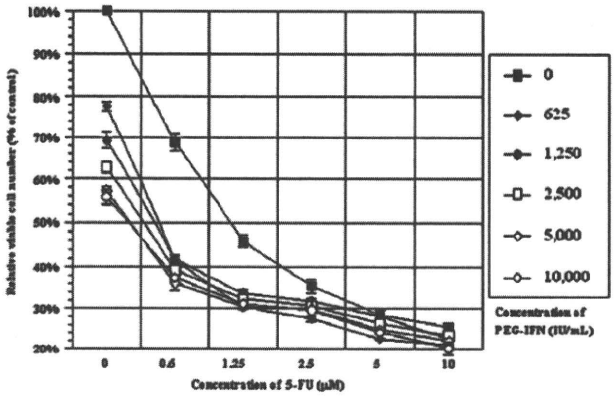

Figure 2. Anti-proliferative effects of the combination therapy of PEG-IFN-α2b and 5-FU on VMRC-RCW cells in a 96-h culture. The relative viable cell number decreased dose-dependently. Two samples were used in each experiment. The experiment was repeated three times. The values represent the average ± SE. PEG-IFN, PEG-IFN-α2b.

calculated the number of artery-like blood vessels in the entire area of each section and obtained for each the mean number per mm^2.

cDNA preparation and quantitative real-time RT-PCR. Total RNA was extracted using RNA-Bee™ (Tel-Test, Inc., TX) and reverse transcribed using Superscript™ III First-Strand Synthesis System for RT-PCR (Invitrogen, CA) according to the manufacturer's instructions. Quantitative real-time RT-PCR was performed with an ABI PRISM 7300 (Applied Biosystems, Foster City, CA). We examined 6 enzymes related to 5-FU metabolism, i.e., TS, TP, DPD, OPRT, UP and TK. The sequences of the primers and probes for the 6 enzymes are listed elsewhere (17). The sequences for VEGF were 5'-CCATGAACTTTCTGCTGTCTTGG-3' as the forward primer, 5'-CTGCGCTGATAGACATCCATGA-3' as the reverse primer, and 5'-TGCTCTACCTCCACCATGC CAAGT-3' as the probe. The sequences of the primers and probes for VEGFR-1, IFNAR-1, IFNAR-2 and glyceraldehyde-3-phosphate dehydrogenase (GAPDH) were purchased from Applied Biosystems.

Statistical analysis. We used two-factorial ANOVA for the comparisons of tumor volume, tumor weight, number of apoptotic cells, number of artery-like blood vessels, and relative levels of mRNAs related to 5-FU metabolism.

Results

Effects of PEG-IFN-α2b on the proliferation of RCC cell lines in vitro. After adding 2,048 IU/ml of PEG-IFN-α2b, the relative viable cell number of the cultured 8 cell lines was suppressed in a time-dependent manner until 72 h, but at 96 h, suppression was noted in only 2 cell lines (KRC/Y and KUR11). On the other hand, with different doses of PEG-IFN-α2b, the relative viable cell number at 96 h was suppressed in the 6 cell lines, i.e., VMRC-RCW, KRC/Y, KURM, KUR11, ACHN and Caki-1. In the 8 cell lines, IC_{50} was not reached for either time- and dose-dependent suppressions, but the most sensitive case was KUR11 with the dose of 2,048 IU/ml at 96 h, i.e., the relative viable cell number was 62.7% of the control (Fig. 1).

In the VMRC-RCW cell line, the anti-tumor effects of PEG-IFN-α2b and IFN-α2b were not markedly different.

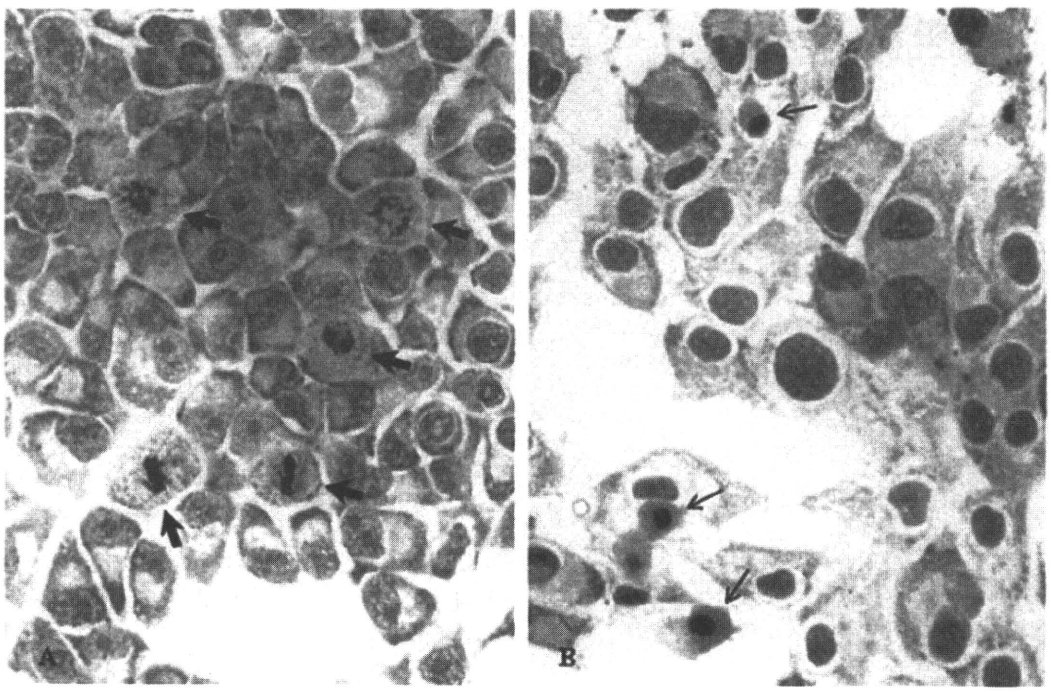

Figure 3. Photomicrograph of VMRC-RCW cells cultured for 72 h on a Lab-Tek Chamber Slide. (A) Without PEG-IFN-α2b in culture medium. Mitotic figures (thick arrows) were noted. (B) With 2.500 IU/m of PEG-IFN-α2b and 2.5 μM of 5-FU in culture medium. Apoptotic cells (thin arrows) characterized by cytoplasmic shrinkage and chromatic condensation were noted (H&E staining, x200).

Table I. Effects of PEG-IFN-α2b and IFN-α2b on RCC cell proliferation in nude mice.

Treatment group	Number	Tumor weight (g, mean ± SE)	Body weight (g, mean ± SE on day 15)
Control (culture medium)	9	1.835±0.132	17.122±0.362
IFN-α2b (640 IU)	9	1.735±0.177	16.089±0.599
IFN-α2b (6,400 IU)	9	1.455±0.140	16.667±0.420
PEG-IFN-α2b (640 IU)	9	1.267±0.072[a,c]	16.156±0.308
PEG-IFN-α2b (6,400 IU)	9	1.160±0.075[b]	15.244±0.313
PEG-IFN-α2b (64,000 IU)	9	0.920±0.126[b]	16.922±0.601
PEG-IFN-α2b (640,000 IU)	8	0.444±0.077[b]	17.638±0.717

Cultured VMRC-RCW cells were subcutaneously transplanted in each nude mouse ($1.0x10^7$/mouse). Seven days later, when the largest diameter of the tumor reached ~10 mm, mice were treated twice per week with s.c. injection of PEG-IFN-α2b, IFN-α2b, or culture medium. All mice were sacrificed on day 15. [a]$p<0.01$ and [b]$p<0.001$ vs. control; [c]$p<0.05$ vs. the same concentration of IFN.

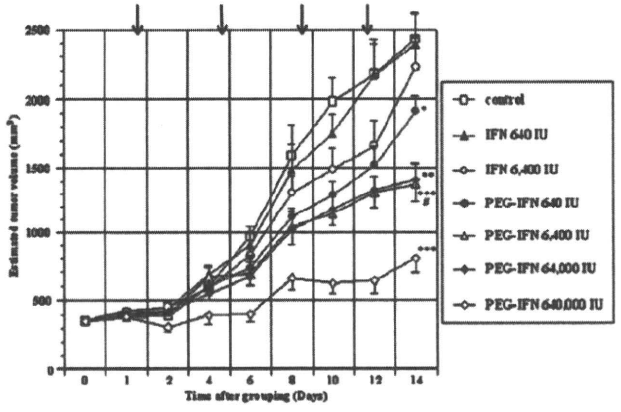

Figure 4. Chronological changes in the estimated volume of subcutaneously transplanted RCC tumors (VMRC-RCW cells, $1.0x10^7$) in nude mice according to the treatment dose. Seven days after the transplantation, when the largest tumor diameter reached ~10 mm (day 0), mice were divided into 7 groups (n=8 or 9, each). The arrows show the days of treatment. *$p<0.05$, **$p<0.01$ and ***$p<0.001$ vs. control; #$p<0.01$ vs. the same dose of IFN-α2b (6,400 IU). The values represent the average ± SE. PEG-IFN, PEG-IFN-α2b.

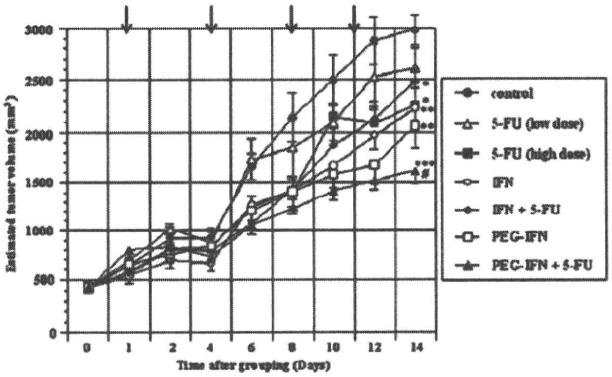

Figure 5. Chronological changes in the estimated volume of subcutaneously transplanted RCC tumors (VMRC-RCW cells, $7.5x10^6$) in nude mice according to the treatment method. Seven days after the transplantation, when the largest tumor diameter reached ~10 mm (day 0), mice were divided into 7 groups (n=8 or 9, each), i.e., PEG-IFN-α2b (6,400 IU) alone; IFN-α2b (6,400 IU) alone; combination of 5-FU and PEG-IFN-α2b (6,400 IU) or IFN-α2b (6,400 IU); 5-FU alone (low or high dose); and culture medium alone (control). The arrows show the days of treatment. *$p<0.05$, **$p<0.01$ and ***$p<0.001$ vs. control; #$p<0.001$ vs. IFN-α2b and 5-FU. The values represent the average ± SE. PEG-IFN, PEG-IFN-α2b.

Effects of the combination treatment of PEG-IFN-α2b and 5-FU on the growth of the VMRC-RCW cell line in vitro. Without 5-FU, the relative viable cell number did not decrease to 50% or lower of the control even when the highest dose of PEG-IFN-α2b (5,000 IU/ml) was added to the culture. When 5-FU (0.6 μM) was used in combination, the relative viable cell number was suppressed to 41.6% even when PEG-IFN-α2b was at the lowest dose (625 IU/ml, Fig. 2). The anti-proliferative effect of these two agents was additive, not synergistic.

Morphological examination in vitro. The 8 cell lines presented such apoptotic features as cytoplasmic shrinkage and chromatin condensation in a varying degree and in a dose-dependent manner at 72 h after adding PEG-IFN-α2b. For the combination treatment of PEG-IFN-α2b and 5-FU, more apoptotic cells were observed than in the PEG-IFN-α2b alone-treated cells, and the apoptotic cells increased dose-dependently to PEG-IFN-α2b plus 5-FU (Fig. 3).

Effects of PEG-IFN-α2b on RCC cell proliferation in nude mice. Chronological changes in estimated tumor volume after IFN administration to nude mice are summarized in Fig. 4. Dose-dependent suppression of tumor volume was observed in mice receiving PEG-IFN-α2b. The estimated tumor volume on day 14 in the mice receiving 6,400 IU of PEG-IFN-α2b became 61.9% of the mice receiving the same dose of IFN-α2b ($p<0.01$) and 56.8% of the control ($p<0.001$). The tumor weight on day 15 in the mice receiving 6,400 IU of PEG-IFN-α2b became 63.2% of the control ($p<0.001$, Table I).

Significant differences in the estimated tumor volume were observed between each PEG-IFN-α2b group (640, 6,400,

Table II. Effects of combination therapy of PEG-IFN-α2b and 5-FU on RCC cell proliferation in nude mice.

Treatment group	Number	Tumor weight (g, mean ± SE)	Body weight (g, mean ± SE on day 15)
Control (culture medium)	8	2.255±0.102	17.188±0.578
5-FU (low dose)	9	2.430±0.185	16.778±0.595
5-FU (high dose)	7	1.603±0.107[c]	15.686±0.814
IFN-α2b alone	8	1.812±0.084[b]	16.363±0.692
IFN-α2b + 5-FU	8	1.917±0.170	16.344±0.426
PEG-IFN-α2b	8	1.771±0.172[a]	15.963±0.459
PEG-IFN-α2b + 5-FU	9	1.742±0.194[a]	15.767±0.621

Cultured VMRC-RCW cells were subcutaneously transplanted in each nude mouse (7.5×10^6/mouse). Seven days later, when the largest diameter of the tumor reached ~10 mm, mice were treated with s.c. injection of IFNs and/or intraperitoneal injection of 5-fluorouracil (5-FU) daily. All mice were sacrificed on day 15. The concentration of both PEG-IFN-α2b and IFN-α2b was 6,400 IU/ml. [a]$p<0.05$, [b]$p<0.01$ and [c]$p<0.001$ vs. control.

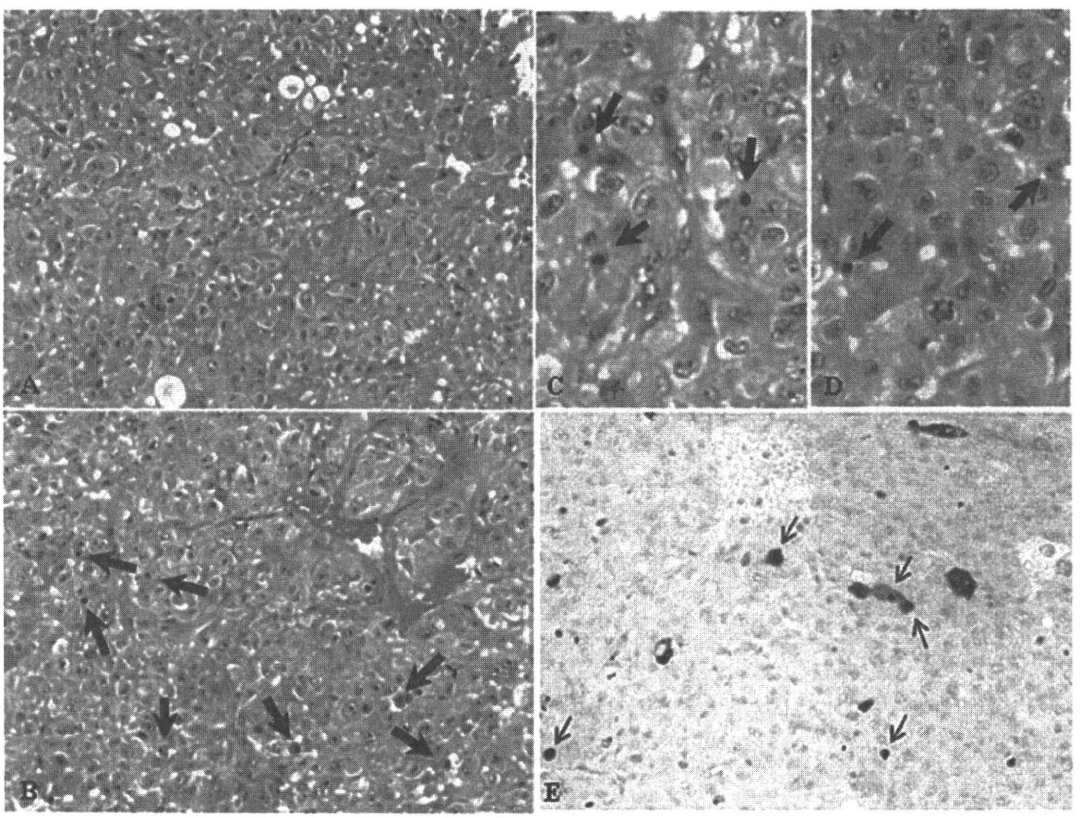

Figure 6. Photomicrograph of a subcutaneous human RCC tumor in nude mice, which developed after the injection of VMRC-RCW cells. (A) A control mouse that received culture medium alone. The tumor showed a thick trabecular arrangement of tumor cells and thin fibrous connective tissues and capillary vessels in the stroma. (B) A mouse that received PEG-IFN-α2b and 5-FU. There were many apoptotic tumor-cells (thick arrows, H&E staining, x200). (C and D) Higher magnifications of B (x400). Apoptotic tumor-cells characterized by shrinkage and eosinophilic change in the cytoplasm and chromatin condensation are shown (thick arrows, H&E staining). (E) TUNEL-positive apoptotic cells showing brown nuclei (thin arrows, TUNEL staining, x200).

64,000, 640,000 IU) and the control ($p<0.05$ to $p<0.001$, Fig. 3). There was no significant difference between 640 or 6,400 IU of the IFN-α2b group and the control. There were no significant differences in body weight of the mice among the groups.

Effects of the combination therapy of PEG-IFN-α2b and 5-FU on RCC cell proliferation in nude mice. Chronological changes in estimated tumor volume are shown in Fig. 5. The tumor volume on day 14 for the combination therapy of PEG-IFN-α2b and 5-FU was 54.2% of the control ($p<0.0001$).

Table III. Relative mRNA expression levels of the enzymes related with 5-FU metabolism, VEGF, VEGFR-1 and type I IFN receptor subunits.

Treatment group	DPD	TP	TK	TS	UP	OPRT	VEGF	VEGFR-1	IFNAR-1	IFNAR-2
5-FU (low dose)	129	101	68	182	59	48	116	135	122	94
5-FU (high dose)	72	50	52	40[a]	86	41	30	93	59	90
IFN-α2b	110	71	82	119	100	103	97	134	108	174
IFN-α2b + 5-FU	95	80	85	74	53	106	56	111	63	44[a,d]
PEG-IFN-α2b	648[b,d]	420[a]	313	297[b,d]	76	124	366[a,d]	277	159	217
PEG-IFN-α2b + 5-FU	159[c]	143[c]	162	129	129	86	251[a,c]	138	91	141

mRNA levels were examined by quantitative real-time RT-PCR and normalized with GAPDH. The values of relative mRNA expression level represent the average of the ratio to the level of control in each group. [a]$p<0.05$ and [b]$p<0.01$ vs. control; [c]$p<0.05$ vs. PEG-IFN-α2b; [d]$p<0.05$ vs. IFN-α2b; and [e]$p<0.01$ vs. IFN-α2b plus 5-FU. DPD, dihydropyrimidine dehydrogenase; TP, thymidine phosphorylase; TK, thymidine kinase; TS, thymidylate synthase; UP, uridine phosphorylase; OPRT, orotate phosphoribosyl transferase; VEGF, vascular endothelial growth factor; VEGFR-1, VEGF receptor 1; IFNAR-1, type I interferon receptor subunit 1; and IFNAR-2, type I interferon receptor subunit 2.

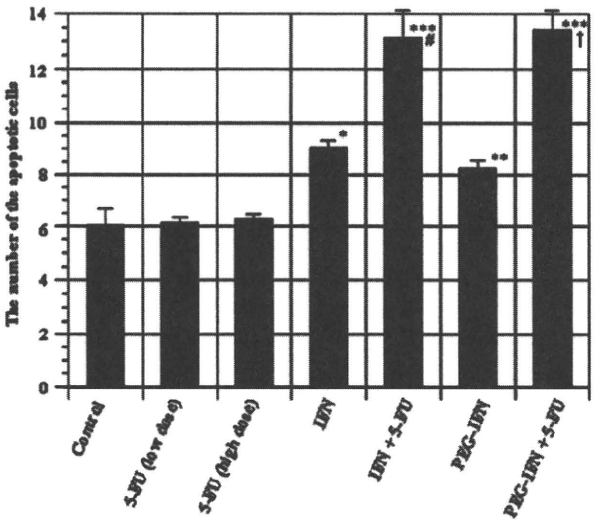

Figure 7. Number of apoptotic cells in the tumors. The number was counted in ten 0.25 mm^2 areas in each section, and the average number per area in each group was obtained. *$p<0.05$, **$p<0.01$ and ***$p<0.001$ vs. control; #$p<0.05$ vs. IFN-α2b; †$p<0.001$ vs PEG-IFN-α2b. PEG-IFN, PEG-IFN-α2b.

The tumor weights of the mice on day 15 were significantly different between the control and the 5-FU high dose group, each IFN alone group, and the combination group of PEG-IFN-α2b and 5-FU. The two types of IFNs and/or 5-FU did not affect the body weight of the mice (Table II).

Histological examination of the RCC tumor specimens stained with H&E revealed that the number of apoptotic cells was significantly higher in the mice treated with 6,400 IU of PEG-IFN-α2b ($p<0.01$) or 6,400 IU of IFN-α2b ($p<0.05$) in comparison to the control (Fig. 6A-D). The incidence of apoptosis in TUNEL-stained sections showed the same tendencies as those obtained in the H&E-stained sections (Fig. 6E). The number of apoptotic cells significantly increased in the mouse tumors treated with the combination therapy in comparison to the control (for each IFN, $p<0.0001$). The number also significantly increased with the combination treatment of PEG-IFN-α2b and 5-FU in comparison to PEG-IFN-α2b alone ($p<0.0001$), and with the combination of IFN-α2b and 5-FU in comparison to IFN-α2b alone ($p<0.05$, Fig. 7).

The results of quantitative real-time RT-PCR are shown in Table III. The VEGF mRNA levels increased significantly in the PEG-IFN-α2b alone group ($p<0.05$ vs. control, $p<0.05$ vs. IFN-α2b) and in the combination (PEG-IFN-α2b plus 5-FU) group ($p<0.05$ vs. control, $p<0.01$ vs. IFN-α2b plus 5-FU). There were also significant increases in the expression levels of DPD ($p<0.01$), TP ($p<0.05$), and TS ($p<0.05$) in the PEG-IFN-α2b alone group in comparison to the control. On the other hand, significant decreases were observed in the expression levels of DPD ($p<0.05$) and TP ($p<0.05$) in the combination (PEG-IFN-α2b plus 5-FU) group in comparison to the PEG-IFN-α2b alone group. In addition, the TS mRNA levels in the PEG-IFN-α2b group increased in comparison to the IFN-α2b group ($p<0.05$). The relative mRNA levels of IFN-α2b receptors in the combination group were lower than the levels of the IFN alone group.

The number of artery-like blood vessels increased slightly in comparison to the control in the groups receiving IFN-α2b alone, PEG-IFN-α2b alone, or the combination therapies; and there were no significant differences among the 7 groups (Fig. 8).

Discussion

Shang *et al* (18) examined 5 RCC cell lines and reported that the greatest decrease in the viable cell number after adding 1,600 IU/ml of Sumiferon to the cultures was 42% (58% of the control). On the other hand, Vyas *et al* (19) comparatively examined the anti-tumor effects of PEG-IFN-α2b and IFN-α2b by using an RCC cell line, ACHN, and reported that the addition of 1,033 IU/ml of PEG-IFN-α2b suppressed the viable cell number to 50% of the control. Our current

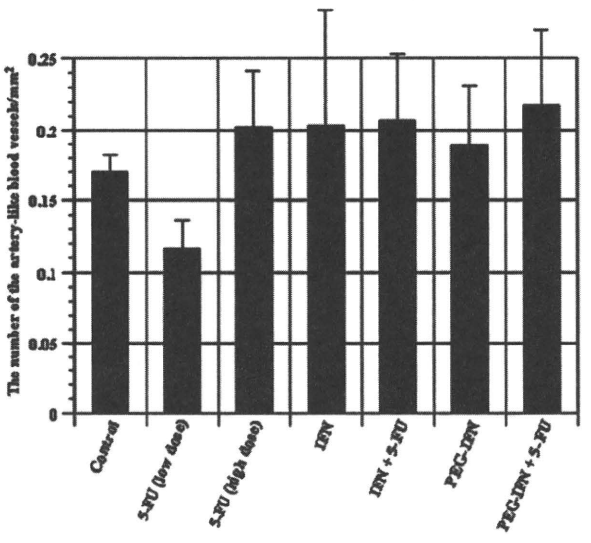

Figure 8. Number of artery-like blood vessels in the tumors. The number was counted in the whole area of each section, and mean number per mm^2 was obtained. Each figure shows the average ± SE. PEG-IFN: PEG-IFN-α2b.

experiment used concentration levels close to those of Shang *et al*, and similar anti-tumor effects were obtained. However, the level of suppression in our study did not reach 50% of the control even though the concentrations were higher than those of Vyas *et al*. The reasons for these disparate findings are not clear, however, they may be related to the different cell density in the experiments, different measurement methods, and possible changes in cell characteristics due to cultures. Vyas *et al* (19) also reported that the anti-tumor effects of PEG-IFN-α2b and IFN-α2b were not markedly different as we demonstrated in the present study.

Some medical institutions administer the combination therapy of IFN-α and 5-FU in the treatment for advanced RCC. Sella *et al* (20) reported that the combination of IFN-α and chemotherapy (5-FU and mitomycin C) resulted in a significant clinical effect on RCC patients. Our results support the anti-tumor effects reported by Sella *et al* regarding the combination of IFN-α and chemotherapy. Moreover, in the present study, the combination of PEG-IFN-α2b and 5-FU exhibited enhanced anti-tumor effects in comparison to the combination of IFN-α2b and 5-FU *in vivo*.

The induction of apoptosis is a mechanism of the anti-tumor effects of IFN-α2b, and Vyas *et al* (19) reported a dose-dependent increase in apoptotic cell number for PEG-IFN-α2b in cell cultures. Shang *et al* (18) found that apoptosis induction by IFN-α2b was not significant even at a dose of 5,000 IU/ml. On the other hand, 5-FU induced apoptosis in a dose-dependent manner, and 50 and 100 IU/ml of IFN-α2b was able to promote 5-FU-induced apoptosis in RCC cells. In our current study, the number of apoptotic cells *in vitro* increased proportionally to the dose of PEG-IFN-α2b and to the doses of PEG-IFN-α2b plus 5-FU in the combination treatment. The apoptotic cell number in the tumors also increased dose-dependently in the IFN-α2b alone group and PEG-IFN-α2b alone group, and the number in each group further increased with the combination of 5-FU. This indicates that PEG-IFN-α2b and IFN-α2b induced apoptosis and the combination with 5-FU induced apoptosis more extensively. Comparing the two combination treatments, i.e., PEG-IFN-α2b plus 5-FU vs. IFN-α2b plus 5-FU, the estimated tumor volume was significantly smaller in the PEG-IFN-α2b plus 5-FU group, but the number of apoptotic cells did not differ markedly between the groups. Shang *et al* (18) revealed that IFN-α2b caused cell cycle arrest at G1 in ACHN cells and at G2/M in Caki-1 cells in their flow cytometric analyses, and this suggests that cell cycle arrest could be the reason why there was no remarkable difference in the number of apoptotic cells in our results.

Anti-angiogenesis activity is a biological effect of IFN-α2b, and it has been shown that IFN-α2b inhibits angiogenesis by down-regulating angiogenesis factors. For example, Dinney *et al* (21) systematically administered IFN-α in a nude mouse model of bladder tumor and reported a decrease in *in vivo* blood vessel density in the tumors, which then resulted in the shrinkage of the tumor size. On the other hand, Kojiro *et al* (16) reported that there was no significant relation between the tumor shrinkage effects and angiogenesis factors or artery-like blood vessels when IFN-α and 5-FU were administered in combination to nude mice receiving transplantation of HCC cells. In our current study, the mRNA expression of VEGF and the number of artery-like blood vessels in the tumors were not suppressed in the PEG-IFN-α2b alone group and the PEG-IFN-α2b plus 5-FU group, but the estimated tumor volume of the PEG-IFN-α2b plus 5-FU group was the most suppressed among the groups. The reason for these contrary findings is unclear. Angiogenesis plays an important role in the proliferation and metastasis of solid tumors such as renal cancer, therefore the relation between angiogenesis factors and anti-tumor effects should be investigated in future studies by using different IFN preparations and other RCC cell lines.

It has been reported that IFN directly suppresses tumor proliferation and at the same time augments the suppressive effects of 5-FU on tumor growth, including the induction of apoptosis (15,22). In regards to the mechanism of this augmentation, several researchers reported that IFN-α acts on the metabolic pathway of 5-FU (23,24). Low levels of TS and DPD and high levels of OPRT, TP, UP and TK render cancer cells sensitive to 5-FU. In our results, the enzymes related to 5-FU metabolism, except OPRT, slightly increased (not significantly) in comparison to the control. Therefore, the activity of 5-FU-related enzymes were not related to the anti-tumor effects shown in our PEG-IFN-α2b plus 5-FU group.

IFN-α2b exerts its actions through a specific cell surface receptor, Type I IFN receptor, which consists of two subunits IFNAR-1 and IFNAR-2. IFNAR-2 is the binding subunit and is more important than IFNAR-1 for the expression of IFN-α2b activity (25-27). Oie *et al* (17) examined the expression of type I IFN receptor mRNA in 6 HCC cell lines treated with 5-FU. They showed that the expression of type I IFN receptor was markedly increased in the 3 cell lines whose proliferation was suppressed synergistically by the administration of 5-FU and IFN-α than in the other 3 cell lines whose proliferation was suppressed in an additive manner. In our current study, expression of IFNAR-1 and IFNAR-2 increased in the IFN-α2b alone and PEG-IFN-α2b alone groups, whereas the expression levels were markedly lower

in the combination groups of IFN-α plus 5-FU than in the IFN alone groups. These findings differ from those of Oie *et al* which could be the reason why the effects of our combination treatment were additive and not synergistic.

Our results confirmed that in the treatment of RCC, PEG-IFN-α2b presents more potent anti-tumor effects than conventional non-pegylated IFN-α2b, and the effects are augmented when 5-FU is used in combination. The most probable mechanism of this potent effect is apoptosis induction, and the target molecules that induce apoptosis will be determined in future studies. We expect that the addition of another agent to the combination of IFN-α2b and 5-FU would result in more potent anti-tumor effects in the treatment of RCC.

Acknowledgements

We thank Ms. Akemi Fujiyoshi for her assistance in our experiments. This study was supported by a Grant-in-Aid from the Ministry of Health, Labor and Welfare of Japan (no. 17200501) and by a Grant-in-Aid for Scientific Research (C) from the Ministry of Education, Science, Sports and Culture, Japan (no. 19590412).

References

1. Hartmann JT and Bokemeyer C: Chemotherapy for renal cell carcinoma. Anticancer Res 19: 1541-1543, 1999.
2. Atzpodien J, Lopez Hanninen E, Kirchner H, Bodenstein H, Pfreundschuh M, Rebmann U, Metzner B, Illiger HJ, Jakse G, Niesel T, *et al*: Multiinstitutional home-therapy trial of recombinant human interleukin-2 and interferon alfa-2 in progressive metastatic renal cell carcinoma. J Clin Oncol 13: 497-501, 1995.
3. Hernberg M, Pyrhonen S and Muhonen T: Regimens with or without interferon-alpha as treatment for metastatic melanoma and renal cell carcinoma: an overview of randomized trials. J Immunother 22: 145-154, 1999.
4. Dutcher JP, Logan T, Gordon M, Sosman J, Weiss G, Margolin K, Plasse T, Mier J, Lotze M, Clark J and Atkins M: Phase II trial of interleukin 2, interferon alpha, and 5-fluorouracil in metastatic renal cell cancer: a cytokine working group study. Clin Cancer Res 6: 3442-3450, 2000.
5. Wadler S and Wiernik PH: Partial reversal of doxorubicin resistance by forskolin and 1, 9-dideoxyforskolin in murine sarcoma S180 variants. Cancer Res 48: 539-543, 1988.
6. Baker DE: Pegylated interferon plus ribavirin for the treatment of chronic hepatitis C. Rev Gastroenterol Disord 3: 93-109, 2003.
7. Reddy KR, Wright TL, Pockros PJ, Shiffman M, Everson G, Reindollar R, Fried MW, Purdum PP III, Jensen D, Smith C, Lee WM, Boyer TD, Lin A, Pedder S and DePamphilis J: Efficacy and safety of pegylated (40-kd) interferon alpha-2a compared with interferon alpha-2a in noncirrhotic patients with chronic hepatitis C. Hepatology 33: 433-438, 2001.
8. Lindsay KL, Trepo C, Heintges T, Shiffman ML, Gordon SC, Hoefs JC, Schiff ER, Goodman ZD, Laughlin M, Yao R and Albrecht JK: A randomized, double-blind trial comparing pegylated interferon alfa-2b to interferon alfa-2b as initial treatment for chronic hepatitis C. Hepatology 34: 395-403, 2001.
9. Lee SD, Yu ML, Cheng PN, Lai MY, Chao YC, Hwang SJ, Chang WY, Chang TT, Hsieh TY, Liu CJ and Chen DS: Comparison of a 6-month course peginterferon alpha-2b plus ribavirin and interferon alpha-2b plus ribavirin in treating Chinese patients with chronic hepatitis C in Taiwan. J Viral Hepat 12: 283-291, 2005.
10. Bruno S, Camma C, Di Marco V, Rumi M, Vinci M, Camozzi M, Rebucci C, Di Bona D, Colombo M, Craxi A, Mondelli MU and Pinzello G: Peginterferon alfa-2b plus ribavirin for naive patients with genotype 1 chronic hepatitis C: a randomized controlled trial. J Hepatol 41: 474-481, 2004.
11. Yano H, Yanai Y, Momosaki S, Ogasawara S, Akiba J, Kojiro S, Moriya F, Fukahori S, Kurimoto M and Kojiro M: Growth inhibitory effects of interferon-alpha subtypes vary according to human liver cancer cell lines. J Gastroenterol Hepatol 21: 1720-1725, 2006.
12. Motzer RJ, Rakhit A, Ginsberg M, Rittweger K, Vuky J, Yu R, Fettner S and Hooftman L: Phase I trial of 40-kd branched pegylated interferon alfa-2a for patients with advanced renal cell carcinoma. J Clin Oncol 19: 1312-1319, 2001.
13. Yano H, Maruiwa M, Sugihara S, Kojiro M, Noda S and Eto K: Establishment and characterization of a new human renal cell carcinoma cell line (KRC/Y). In Vitro Cell Dev Biol 24: 9-16, 1988.
14. Hisaka T, Yano H, Ogasawara S, Momosaki S, Nishida N, Takemoto Y, Kojiro S, Katafuchi Y and Kojiro M: Interferon-alphaCon1 suppresses proliferation of liver cancer cell lines in vitro and in vivo. J Hepatol 41: 782-789, 2004.
15. Chou T-C and Talalay P: Analysis of combined drug effects: a new look at a very old problem. Trends Pharmacol Sci 4: 450-454, 1983.
16. Kojiro S, Yano H, Ogasawara S, Momosaki S, Takemoto Y, Nishida N and Kojiro M: Antiproliferative effects of 5-fluorouracil and interferon-alpha in combination on a hepatocellular carcinoma cell line in vitro and in vivo. J Gastroenterol Hepatol 21: 129-137, 2006.
17. Oie S, Ono M, Yano H, Maruyama Y, Terada T, Yamada Y, Ueno T, Kojiro M, Hirano K and Kuwano M: The up-regulation of type I interferon receptor gene plays a key role in hepatocellular carcinoma cells in the synergistic antiproliferative effect by 5-fluorouracil and interferon-α. Int J Oncol 29: 1469-1478, 2006.
18. Shang D, Ito N, Watanabe J, Awakura Y, Nishiyama H, Kamoto T and Ogawa O: Synergy of interferon-alpha and 5-fluorouracil in human renal cell carcinoma requires p53 activity. Eur Urol 52: 1131-1139, 2007.
19. Vyas K, Brassard DL, DeLorenzo MM, Sun Y, Grace MJ, Borden EC and Leaman DW: Biologic activity of polyethylene glycol 12000-interferon-alpha2b compared with interferon-alpha2b: gene modulatory and antigrowth effects in tumor cells. J Immunother 26: 202-211, 2003.
20. Sella A, Logothetis CJ, Fitz K, Dexeus FH, Amato R, Kilbourn R and Wallace S: Phase II study of interferon-alpha and chemotherapy (5-fluorouracil and mitomycin C) in metastatic renal cell cancer. J Urol 147: 573-577, 1992.
21. Dinney CP, Bielenberg DR, Perrotte P, Reich R, Eve BY, Bucana CD and Fidler IJ: Inhibition of basic fibroblast growth factor expression, angiogenesis, and growth of human bladder carcinoma in mice by systemic interferon-alpha administration. Cancer Res 58: 808-814, 1998.
22. Oka Y, Naomoto Y, Yasuoka Y, Hatano H, Haisa M, Tanaka N and Orita K: Apoptosis in cultured human colon cancer cells induced by combined treatments with 5-fluorouracil, tumor necrosis factor-alpha and interferon-alpha. Jpn J Clin Oncol 27: 231-235, 1997.
23. Kase S, Kubota T, Watanabe M, Teramoto T, Kitajima M and Hoffman RM: Recombinant human interferon alpha-2a increases 5-fluorouracil efficacy by elevating fluorouridine concentration in tumor tissue. Anticancer Res 14: 1155-1159, 1994.
24. Schwartz EL, Hoffman M, O'Connor CJ and Wadler S: Stimulation of 5-fluorouracil metabolic activation by interferon-alpha in human colon carcinoma cells. Biochem Biophys Res Commun 182: 1232-1239, 1992.
25. Pestka S, Langer JA, Zoon KC and Samuel CE: Interferons and their actions. Annu Rev Biochem 56: 727-777, 1987.
26. Lutfalla G, Holland SJ, Cinato E, Monneron D, Reboul J, Rogers NC, Smith JM, Stark GR, Gardiner K, Mogensen KE, *et al*: Mutant U5A cells are complemented by an interferon-alpha beta receptor subunit generated by alternative processing of a new member of a cytokine receptor gene cluster. EMBO J 14: 5100-5108, 1995.
27. Domanski P, Witte M, Kellum M, Rubinstein M, Hackett R, Pitha P and Colamonici OR: Cloning and expression of a long form of the beta subunit of the interferon alpha beta receptor that is required for signaling. J Biol Chem 270: 21606-21611, 1995.

N-myc downstream regulated gene 1 (NDRG1)/Cap43 enhances portal vein invasion and intrahepatic metastasis in human hepatocellular carcinoma

JUN AKIBA[1,2], SACHIKO OGASAWARA[1,2], AKIHIKO KAWAHARA[2,3], NAOYO NISHIDA[1,2], SAKIKO SANADA[1,2], FUKUKO MORIYA[1,2], MICHIHIKO KUWANO[2], OSAMU NAKASHIMA[1,2] and HIROHISA YANO[1,2]

[1]Department of Pathology, Kurume University School of Medicine, [2]Research Center of Innovative Cancer Therapy of the 21 Century COE Program for Medical Science, [3]Department of Pathology, Kurume University Hospital, 67 Asahi-machi, Kurume, Fukuoka 830-0011, Japan

Received June 12, 2008; Accepted September 5, 2008

DOI: 10.3892/or_00000148

Abstract. N-myc downstream regulated gene 1 (NDRG1)/Cap43 is a 43 kDa protein that is widely distributed in the body. Its expression is regulated by nickel, cobalt, hypoxic condition and others; it is reported to be weaker in tumors than normal tissues; and NDRG1/Cap43 is considered to act suppressively to tumor metastasis. This current study immunohistochemically examined NDRG1/Cap43 expression in hepatocellular carcinoma (HCC), and analyzed its relationship to clinicopathologic factors and prognosis. The samples were 105 surgically resected HCC tissue blocks, i.e., 18 well-differentiated HCC, 61 moderately differentiated HCC, 10 poorly differentiated HCC, 9 'nodule-in-nodule' type HCC, and 7 sarcomatous HCC. In all cases, NDRG1/Cap43 was not expressed in normal liver cells. Strong expression was found in 65 of the 105 cases (62%), i.e., in 11.1% of well-differentiated HCC, 72.1% of moderately differentiated HCC, 80.0% of poorly differentiated HCC, and 71.4% of sarcomatous HCC. In the 'nodule-in-nodule' type, its expression was found in 55.6% of their well-differentiated component, and this frequency was significantly higher than that in well-differentiated HCC (11.1%). In the cases showing strong NDRG1/Cap43 expression, frequency of portal vein invasion and of intrahepatic metastasis was significantly high. No clear relationship between the expression and prognosis was observed. NDRG1/Cap43 expression that was found in advanced HCC was thought to accelerate tumor invasion and metastasis. NDRG1/Cap43 could act as a useful biomarker of HCC.

Correspondence to: Dr Jun Akiba, Department of Pathology, Kurume University School of Medicine, 67 Asahi-machi, Kurume, Fukuoka 830-0011, Japan
E-mail: akiba@med.kurume-u.ac.jp

Key words: N-myc, Cap43, hepatocellular carcinoma

Introduction

Hepatocellular carcinoma (HCC) is the fifth commonest malignancy worldwide and is the third most common cause of cancer related death. The geographic areas at highest risk are located in Eastern Asia, Middle Africa, and some countries of Western Africa. HCC most commonly develops in patients with chronic liver disease, the etiology of which includes alcohol, viral infection (hepatitis B and C), metabolic diseases and aflatoxin (1,2). Surgery, including transplantation, remains the only curative modality for HCC. The prognosis of HCC is generally poor, and even after surgery, the 5-year survival rate is limited to 25-29% (3). The ability to predict patients at higher risk of recurrence and with a poor prognosis would help to guide surgical and chemotherapeutic treatment. Efforts have been made to predict recurrence and poor prognosis in patients with HCC after hepatectomy using clinicopathological parameters. Tumor size, tumor number, vascular invasion and the presence of satellite lesion were reported to be useful predictors (4-6). With the development of molecular biology, many biomarkers related to invasion, metastasis, recurrence and survival have been explored.

N-myc downstream regulated gene 1 (NDRG1, also known as Drd-1, Cap43 or RTP) was identified as a homocysteine-responsive gene that was induced by sulfhydryl regents such as cysteine and 2-mercaptoethanol in human umbilical vein endothelial cells (7). The NDRG1/Cap43 gene is mapped to chromosome 8q24 (8) and encodes a 3.0 kb mRNA that is translated into a protein with a molecular weight of 43 kDa (7,9). NDRG1/Cap43 expression is regulated with nickel, cobalt, oxidative stress, hypoxia, phorbol esters, vitamin A and D, steroids, histone deacetylase-targeting drugs, lysophosphatidylcholine, oncogene, and tumor suppressor gene (p53 and VHL) products (7,8,10-12). NDRG1/Cap43 acts in maintenance and differentiation (13) of myelin sheath; and in exocytosis (14), maturation (15) and degranulation (16) of mast cells. The NDRG1/CAP43 mRNA is widely expressed in the non-neoplastic tissues and its expression is especially high in the prostate (17), brain (18), kidney (13,19), placenta and

intestine (1,3,4,7,9,10,14,15,20,21). Sincce NDRG1/Cap43 expression level in neoplastic cells of breast cancer, prostatic cancer and colon cancer is lower in comparison to that in non-neoplastic tissues, NDRG1/Cap43 is reported to be suppressive to tumor metastasis (8,9,17,22-24). On the other hand, NDRG1/Cap43 is also reported to be overexpressed in tumor tissue than normal tissue (25), and to act as an accelerating factor of metastasis (26). At present, actions of NDRG1/Cap43 in tumor remain elusive.

To date, NDRG1/Cap43 expression in the liver (25) and its relationship with hepatocellular carcinoma (HCC) were reported (27,28). Chua *et al* showed high NDRG1/Cap43 expression in HCC correlated with shorter overall survival, late tumor stage, vascular invasion, large tumor size, and high histological grade and NDRG1/Cap43 could be a useful predictor (27). In the current study we investigated NDRG1/Cap43 expression and its histopathological features on surgically resected HCC of humans, and evaluated NDRG1/Cap43 as a possible biomarker of HCC.

Materials and methods

Tissue samples. Immunohistochemical examination was performed on formalin-fixed paraffin sections of cancerous and non-cancerous tissues of 105 HCC livers that were surgically resected at Kurume University Hospital in the period between 1989 and 2007. The 105 patients did not receive preoperative anticancer therapies such as a trans-catheter arterial embolization and radiofrequency are summarized in Table I. Among them, 89 cases had a nodule

Table I. Clinicopathological characteristics of 105 HCC cases.

Clinicopathological factors	No. of cases (%)
Age (years, mean ± SD)	64.3±8.5
Sex (M/F)	80/25
Tumor size (mm, mean ± SD)	38.2±25.2
Differentiation	
Well-differentiated	18 (17.1)
Moderately differentiated	61 (58.1)
Poorly differentiated	10 (9.5)
HCC with sarcomatous change	7 (6.7)
Nodule-in-nodule appearance	9 (8.6)
Portal vein invasion	46 (43.8)
Venous invasion	7 (6.7)
Bile duct invasion	4 (3.8)
Intrahepatic metastasis	8 (26.7)
Virus marker	
Hepatitis B virus (HBV) associated	10 (9.5)
Hepatitis C virus (HCV) associated	75 (71.4)
HBV and HCV associated	9 (8.6)
HBV and HCV negative	6 (5.7)
Unknown	5 (4.8)

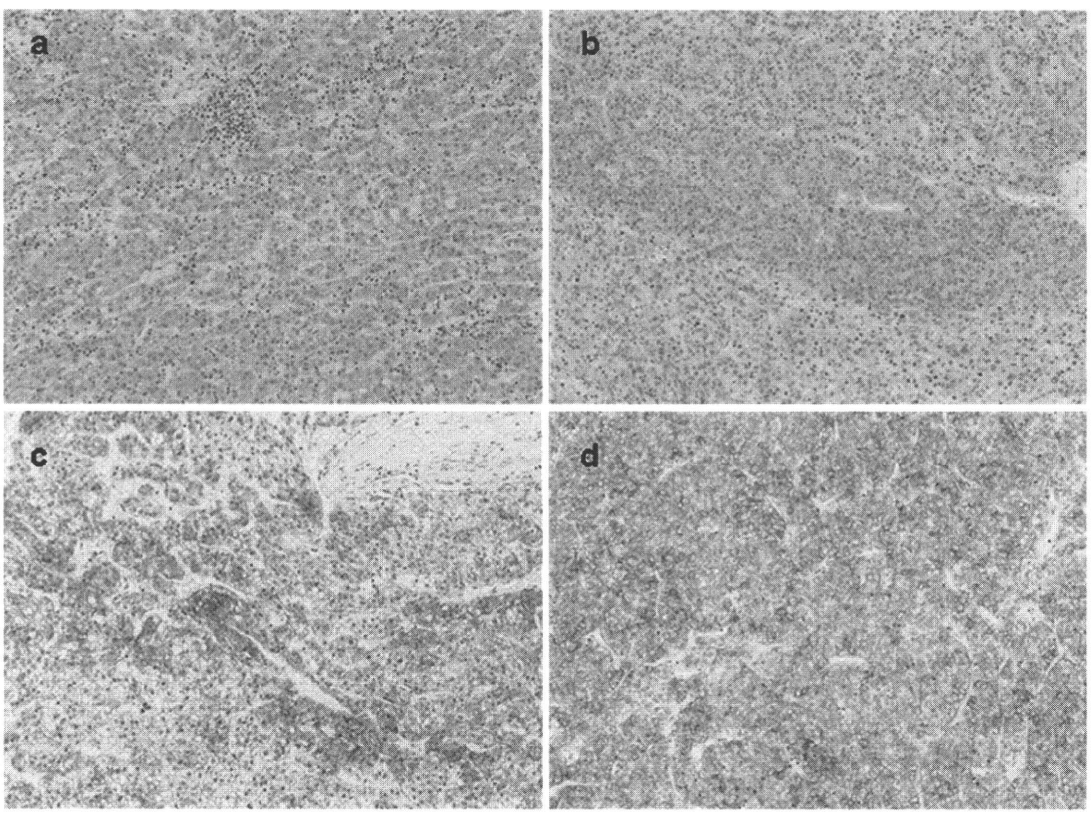

Figure 1. Grading of NDRG1/Cap43 staining distribution. (a) Grade 0: NDRG1/CAP43 positive cells were present <10% of the entire area. (b) Grade +1: the area was 10-40%. (c) Grade +2: the area was 40-70%. (d) Grade +3: the area was 70-100%.

Table II. Relationship between NDRG1/Cap43 expressions and clinicopathological factors.

Clinicopathological factors		NDRG1/Cap43 expression		p value (χ^2 test)
		Strong (n=65)	Weak (n=40)	
Age (years, mean ± SD)		63.8±9.3	65.1±7.2	NS
Gender	Male	48	32	NS
	Female	17	8	
Tumor size (mm, mean ± SD)			41.3±22.9	33.4±28.4
NS				
Histological grade				
Well-differentiated[(a)]		2	16	
Moderately differentiated		44	17	p<0.0001, vs. (a)
Poorly differentiated		8	2	p=0.0003, vs. (a)
HCC with sarcomatous change		5	2	p=0.0032, vs. (a)
Nodule-in-nodule appearance				
Well-differentiated component		5	4	p=0.0145, vs. (a)
Moderately differentiated component		6	3	p=0.003, vs. (a)
Portal vein invasion	(+)	37	9	p=0.0004
	(-)	28	31	
Venous vein invasion	(+)	6	1	NS
	(-)	59	39	
Bile duct invasion	(+)	4	1	NS
	(-)	61	39	
Intrahepatic metastasis	(+)	23	5	p=0.0074
	(-)	42	35	
Hepatitis B virus	(+)	15	4	NS
	(-)	50	36	
Hepatitis C virus	(+)	49	35	NS
	(-)	16	5	

of single histological grade, i.e., 18 well-differ-entiated HCC, 61 moderately differentiated HCC, and 10 poorly differentiated HCC. Another 9 cases had 2 different histological grades in a single tumor nodule, i.e., well-differentiated component and moderately differentiated component with a clear boundary between them ('nodule-in-nodule' type). The remaining 7 cases presented sarcomatous changes (sarcomatous HCC). Pathological features of HCC were evaluated according to the World Health Organization (WHO) classification (29).

Immunohistochemistry. Formalin-fixed, paraffin-embedded sections (4 μm) were mounted on 3-aminoprophl-triethoxysilane-coated slides (Matsunami Glass Inc., Ltd., Osaka, Japan), deparaffinized in xylene, and re-hydrated in graded alcohol. The sections were soaked in 10 mmol/l of sodium citrate buffer (pH 6.0) and treated in microwave for 20 min for antigen retrieval. NDRG1/Cap43 expression was immunohistochemically examined with rabbit polyclonal anti-NDRG1/Cap43 antibody (gift from Professor K. Kohno, Department of Molecular Biology, University of Occupation and Environmental Health, Fukuoka, Japan. Diluted 1:2000) as the primary antibody (12,30), and using Histofine SAB-PO kit (Nichirei, Tokyo, Japan) according to the manufacturer's protocol. The sections were incubated with primary antibody for 60 min at room temperature after blocking endogenous biotin and peroxidase activities. Negative control was prepared by replacing the primary antibody with normal rabbit serum. The peroxidase reaction was developed with the addition of 3, 3-diaminobenzidine and H_2O_2 substrate solution. After counterstaining with hematoxylin, the slides were dehydrated, coverslipped, and observed under a microscope (Olympus BX41, Olympus Optical, Tokyo, Japan). The immunohistochemical staining was evaluated independently by two pathologists (J.A. and H.Y.). Immunoreactivity of NDRG1/Cap43-positive cells was compared among the tissue sections, and the ratio of the area where positive cells were present to the area of entire specimen was calculated. NDRG1/Cap43

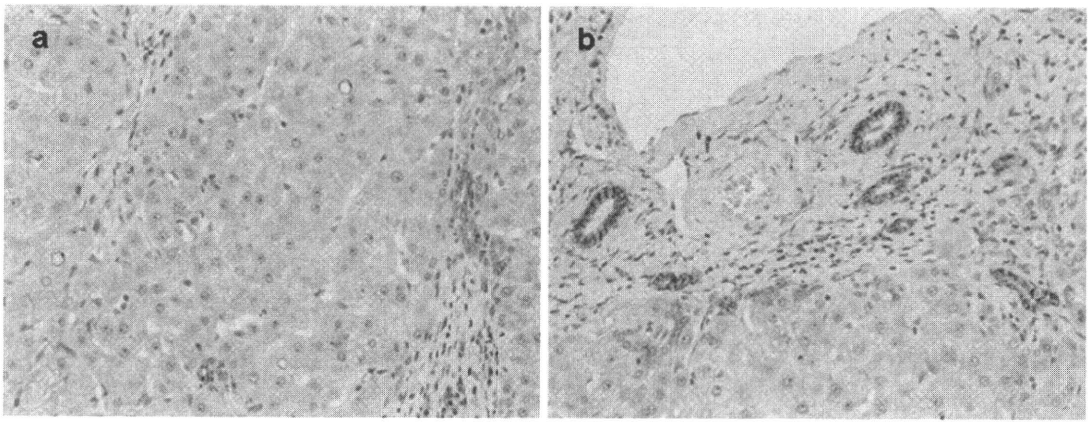

Figure 2. NDRG1/Cap43 expression in non-neoplastic tissues. (a) NDRG1/Cap43 was always negative in normal liver cells. (b) Bile duct epithelium in portal tract was always positive.

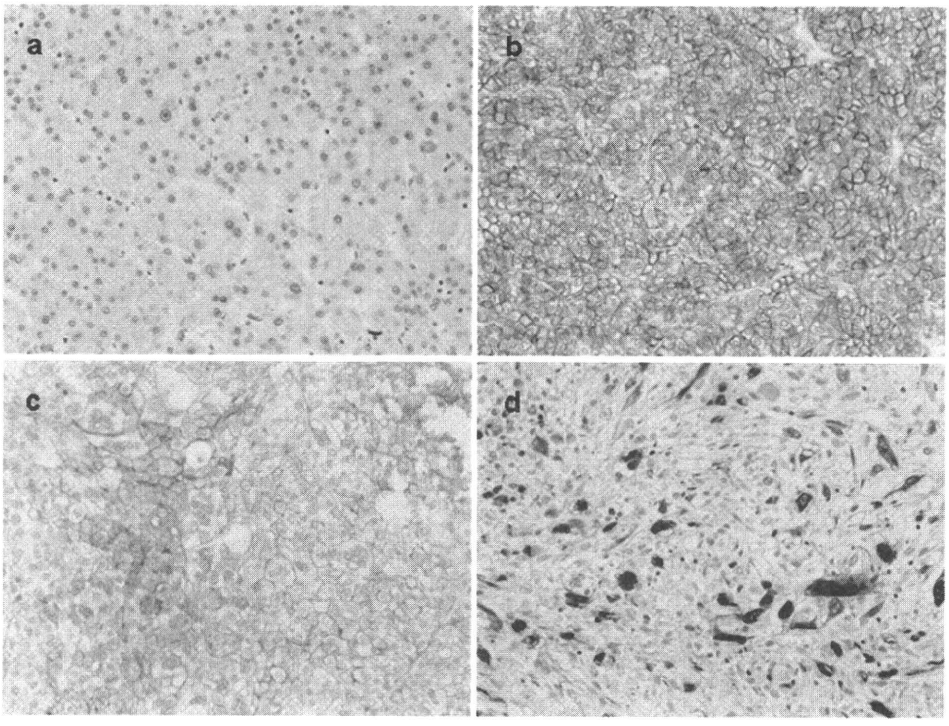

Figure 3. Photomicrograph of immunohistochemical staining. (a) NDRG1/Cap43 in well-differentiated HCC, (b) in moderately differentiated HCC, (c) in poorly differentiated HCC, (d) in HCC with sarcomatous change.

expression in bile duct epithelium was used as an internal positive control because it is always positive. NDRG1/Cap43 expression was graded into 4 levels according to the distribution of immunoreactive HCC cells (Fig. 1), i.e., 0 when NDRG1/Cap43-positive cells were present in <10% of the entire area, +1 when the area was 10-40%, +2 when 40-70%, and +3 when 70-100%. Staining intensity for NDRG1/Cap43 was graded into 3 levels, i.e., 0 when the intensity in HCC area was less than that of bile duct epithelium, +1 when the intensity was almost equal to that of bile duct epithelium, and +2 when the intensity was stronger than that of bile duct epithelium. Total score was obtained as the expression grade multiplied by the staining intensity score. This total score was then evaluated into 2 levels, i.e., 0-2, weak expression; 3-6, strong expression, and the relationship between NDRG1/Cap43 expression and clinicopathological features was examined. Statistical significance was examined with χ^2 test.

The relationship between NDRG1/Cap43 expression and postoperative course was examined in 72 of 105 cases who were monitored up to 9.1 years after surgery. The survival rates were calculated by using the Kaplan-Meier method, and the differences were compared by the log-rank test.

Results

NDRG1/Cap43was always negative in non-cancerous liver cells, and its positivity was not affected by the condition of

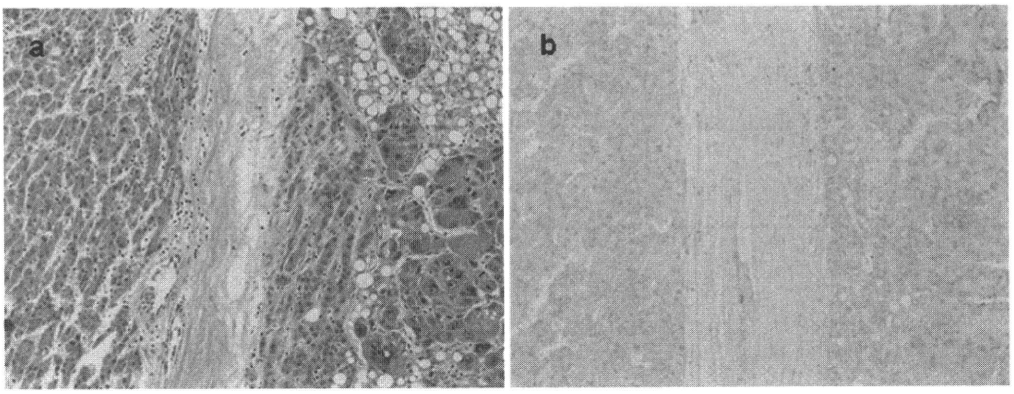

Figure 4. Photomicrographs. (a) The boundary between well-differentiated component (left) and moderately differentiated component (right) with a nodule-in-nodule appearance. (b) NDRG1/Cap43 was immunohistochemically stained in well-differentiated component (left) and moderately differentiated component (right).

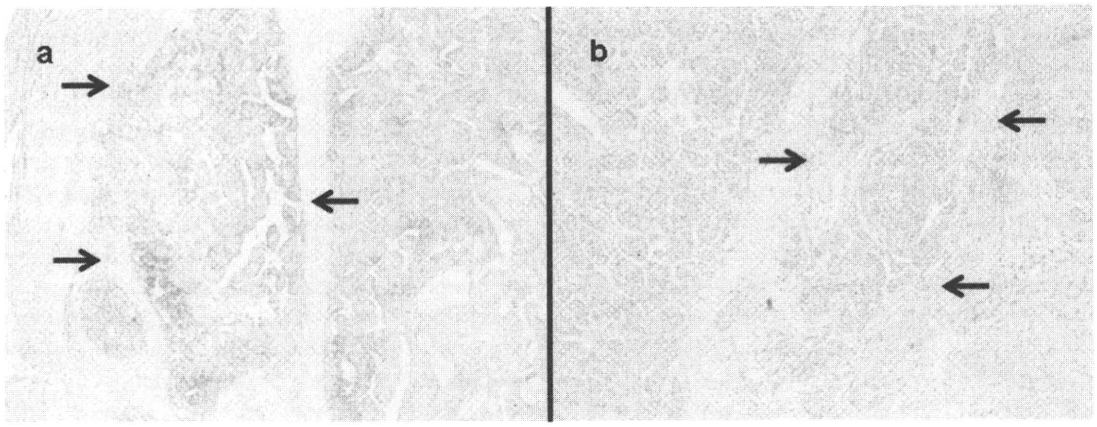

Figure 5. The area of portal vein invasion. (a) Strong NDRG1/Cap43 expression was found in tumor body and in the tumor casts of portal vein (arrows). (b) In one case, NDRG1/Cap43 expression was not found tumor body and in the tumor casts of portal vein (arrows).

the liver (e.g., hepatitis and cirrhosis) or the type of infected hepatitis virus. On the other hand, NDRG1/Cap43 was always positive on the bile duct membrane in the portal tract (Fig. 2), and this picture was used as the internal positive control in this study. Among the 105 cases, NDRG1/Cap43 was expressed at a high level in 65 (62.0%) cases. Their cytoplasm and/or cellular membrane were NDRG1/Cap43 positive, but nuclei were not. There was no significant relationship between the location of positively stained area and clinicopathologic factors. In the 89 cases that HCC nodules were in a single histological grade, strong NDRG1/Cap43 expression was found in 11.1% (2/18) of the well-differentiated HCC, 72.1% (44/61) of moderately differentiated HCC ($p<0.0001$, vs. well-differentiated), and 80.0% (8/10) of the poorly differentiated HCC ($p=0.0003$) (Table II). Among the 7 sarcomatous HCC cases, strong NDRG1/Cap43 expression was observed in 5 (71.4%) and this was significantly higher than the well-differentiated HCC ($p=0.0032$, Fig. 3). In the 9 cases with 'nodule-in-nodule' appearance that contained 2 or more components of different histological grades, NDRG1/Cap43 was strongly expressed in 55.6% (5/9) of well-differentiated component and 66.7% (6/9) of moderately differentiated component (Table II). The frequency in well-differentiated component was significantly higher than that in the well-differentiated HCC of a single histological grade ($p=0.0145$, Fig. 4). In the relationship with clinicopathologic factors, frequencies of portal vein invasion and intrahepatic metastasis were significantly high in the cases of strong NDGR1/Cap43 expression ($p=0.0004$ and $p=0.0074$, respectively). Among the 17 cases who were evaluable for NDRG1/Cap43 expression in the tumor casts of portal vein, 16 cases showed strong expression in the entire tumor body as well as in the tumor casts of portal vein, but one of the 17 cases showed low expression in the tumor body as well as in the tumor casts of portal vein (Fig. 5). Post-operative course was monitored in 72 cases, and NDRG1/Cap43 expression was not clearly related to their survival time. However, among clinicopathological factors the presence of portal vain invasion was significantly associated with shorter survival (log-rank test; $p=0.003$) and intrahepatic metastasis also influenced shorter survival (log-rank test; $p=0.0575$) (Fig. 6).

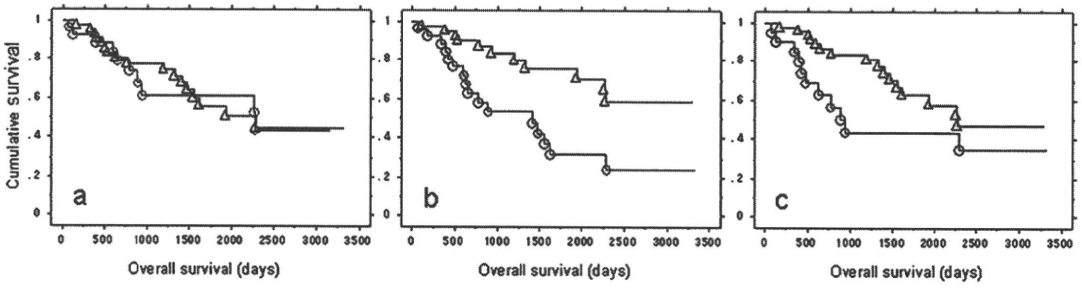

Figure 6. Kaplan-Meier analysis for overall survival time. (a) There was no significant difference between HCC with strong NDRG1/Cap43 expression (Δ) and HCC with weak NDRG1/Cap43 expression (○). (b) Significant difference was observed between HCC with portal vein invasion (○) and HCC without portal vein invasion (Δ) (log-rank test; p=0.003). (c) The period tended to be shorter in cases with intrahepatic metastasis (○) than those without intrahepatic metastasis (Δ) (log-rank test; p=0.0575).

Discussion

Cangul (25) reported no or very mild positivity in non-neoplastic liver cells. Chua *et al* (27) found no NDRG1/Cap43 expression in normal liver cells, but 6% of cirrhosis and benign liver lesions had the expression. On the other hand, in our cases, NDRG1/Cap43 was not expressed in non-neoplastic liver cells even though many of our cases were positive to hepatitis B and/or C virus and had conditions of chronic hepatitis or cirrhosis. This difference in the findings would be attributable to the differences of antibody and immunostaining kits used in each study, disease condition of the patients examined, and evaluation method. Since it was not expressed in non-neoplastic liver cells but shown with the development of tumor, NDRG1/Cap43 could be a marker of HCC.

NDRG1/Cap43 was strongly expressed in 62.0% of the lesions of our cases, and the frequency of strong expression was significantly higher in the moderately and poorly differentiated HCC in comparison to well-differentiated HCC. This indicated that NDRG1/Cap43 is not related to early event of carcinogenesis in the liver but to the growth and development into advanced HCC. This point is supported by the findings that the cases with strong NDRG1/Cap43 expression highly associated with portal vein invasion or intrahepatic metastasis, and tended to have a larger diameter of the nodule. The relationship between NDRG1/Cap43 expression and cancer has not yet been fully elucidated, but previous studies reported that NDRG1/Cap43 acts suppressively to metastasis in prostatic cancer, breast cancer, colon cancer and pancreatic cancer; and is also a useful prognostic factor (22-24,31). In our current study, the relationship between NDRG1/Cap43 and prognosis was not clear, but the results indicated that NDRG1/Cap43 accelerates vascular invasion and metastasis of cancer. Chua *et al* (27) also showed in their HCC study that NDRG1/Cap43 is an indicator of poor prognosis and related to such features as vascular invasion, large tumor size and high histological grade. On the other hand, in our cases portal vain invasion and intrahepatic metastasis was associated with short survival, and frequencies of portal vain invasion and intrahepatic metastasis was significantly high in the cases with NDRG1/Cap43 high expression. This suggests NDRG1/Cap43 high expression is indirectly associated with short survival.

HCC develops in the liver with such chronic diseases as hepatitis and cirrhosis. It occurs as a well-differentiated cancer without having a capsule or distinct margin, and then de-differentiate to present 'nodule-in-nodule' appearance that contains moderately or poorly differentiated component within the nodule. At that stage, tumor growth is accelerated. In our findings, frequencies of NDRG1/Cap43 expression in the well-differentiated component of a 'nodule-in-nodule' type HCC was higher than in a well-differentiated HCC that consists of a single grade HCC. In our cases, NDRG1/Cap43 may act as a promoter of dedifferentiation. Another possible explanation for this difference in the expression rates is that we examined well-differentiated HCC that was in the early-stage of development, contained a single nodule of a single histological grade, and had indistinct margin; therefore the environment such as vascular structure is different from that of 'nodule-in-nodule' type HCC resulting in a different staining pattern to NDRG1/Cap43 even when their histological grade was the same as the corresponding component in a 'nodule-in-nodule' type HCC.

Vascular structure of HCC changes from portal vein to arterial vessel along with tumor growth, and in this course ischemic condition temporally occurs (32). On the other hand, NDRG1/Cap43 expression is upregulated in hypoxia in several cancer types (19,25,28,33) including HCC (28). In our current study, not many of our well-differentiated nodules, i.e., the early-stage HCC, expressed NDRG1/Cap43, whereas the well-differentiated component of 'nodule-in-nodule' type that would be under hypoxic stress in its growth process expressed NDRG1/Cap43 at a high frequency. This suggests that hypoxia would be one of the factors that regulate NDRG1/Cap43 expression in HCC.

Many of our cases that showed strong NDRG1/Cap43 expression in the area of portal tract invasion also showed strong expression in the tumor body. On the other hand, there was no expression in the area of portal tract invasion in the cases that showed weak expression in the tumor body. HCC with strong NDRG1/Cap43 expression had significantly high frequency of portal tract invasion, and they also showed NDRG1/Cap43 expression in the area around the invasion. This indicated a mechanism where NDRG1/Cap43-positive cells with high invasive capability invaded the portal tract and then started to express NDRG1/Cap43.

Our findings showed that NDRG1/Cap43 expression occurs in developed HCC and it promotes invasion and metastasis. More details of the mechanism that accelerates proliferation and metastasis should be examined in future studies.

Acknowledgements

We gratefully thank Ms. Sachiyo Maeda, Akiko Tanaka, Akemi Fujiyoshi and Misato Shiraishi for their excellent technical assistance.

References

1. Yamamoto J, Kosuge T, Takayama T, Shimada K, Yamasaki S, Ozaki H, Yamaguchi N and Makuuchi M: Recurrence of hepatocellular carcinoma after surgery. Br J Surg 83: 1219-1222, 1996.
2. Chen XP, Qiu FZ, Wu ZD, Zhang ZW, Huang ZY and Chen YF: Long-term outcome of resection of large hepatocellular carcinoma. Br J Surg 93: 600-606, 2006.
3. Kondo M, Yamamoto H, Nagano H, Okami J, Ito Y, Shimizu J, Eguchi H, Miyamoto A, Dono K, Umeshita K, Matsuura N, Wakasa K, Nakamori S, Sakon M and Monden M: Increased expression of COX-2 in nontumor liver tissue is associated with shorter disease-free survival in patients with hepatocellular carcinoma. Clin Cancer Res 5: 4005-4012, 1999.
4. Hanazaki K, Kajikawa S, Koide N, Adachi W and Amano J: Prognostic factors after hepatic resection for hepatocellular carcinoma with hepatitis C viral infection: univariate and multivariate analysis. Am J Gastroenterol 96: 1243-1250, 2001.
5. Yeh CN, Chen MF, Lee WC and Jeng LB: Prognostic factors of hepatic resection for hepatocellular carcinoma with cirrhosis: univariate and multivariate analysis. J Surg Oncol 81: 195-202, 2002.
6. Tsai TJ, Chau GY, Lui WY, Tsay SH, King KL, Loong CC, Hsia CY and Wu CW: Clinical significance of microscopic tumor venous invasion in patients with resectable hepatocellular carcinoma. Surgery 127: 603-608, 2000.
7. Kokame K, Kato H and Miyata T: Homocysteine-respondent genes in vascular endothelial cells identified by differential display analysis. GRP78/BiP and novel genes. J Biol Chem 271: 29659-29665, 1996.
8. Kurdistani SK, Arizti P, Reimer CL, Sugrue MM, Aaronson SA and Lee SW: Inhibition of tumor cell growth by RTP/rit42 and its responsiveness to p53 and DNA damage. Cancer Res 58: 4439-4444, 1998.
9. van Belzen N, Dinjens WN, Diesveld MP, Groen NA, van der Made AC, Nozawa Y, Vlietstra R, Trapman J and Bosman FT: A novel gene which is up-regulated during colon epithelial cell differen-tiation and down-regulated in colorectal neoplasms. Lab Invest 77: 85-92, 1997.
10. Zhou D, Salnikow K and Costa M: Cap43, a novel gene specifically induced by $Ni2^+$ compounds. Cancer Res 58: 2182-2189, 1998.
11. Shimono A, Okuda T and Kondoh H: N-myc-dependent repression of ndr1, a gene identified by direct subtraction of whole mouse embryo cDNAs between wild type and N-myc mutant. Mech Dev 83: 39-52, 1999.
12. Masuda K, Ono M, Okamoto M, Morikawa W, Otsubo M, Migita T, Tsuneyoshi M, Okuda H, Shuin T, Naito S and Kuwano M: Downregulation of Cap43 gene by von Hippel-Lindau tumor suppressor protein in human renal cancer cells. Int J Cancer 105: 803-810, 2003.
13. Okuda T, Higashi Y, Kokame K, Tanaka C, Kondoh H and Miyata T: Ndrg1-deficient mice exhibit a progressive demyelinating disorder of peripheral nerves. Mol Cell Biol 24: 3949-3956, 2004.
14. Sugiki T, Murakami M, Taketomi Y, Kikuchi-Yanoshita R and Kudo I: N-myc downregulated gene 1 is a phosphorylated protein in mast cells. Biol Pharm Bull 27: 624-627, 2004.
15. Sugiki T, Taketomi Y, Kikuchi-Yanoshita R, Murakami M and Kudo I: Association of N-myc downregulated gene 1 with heat-shock cognate protein 70 in mast cells. Biol Pharm Bull 27: 628-633, 2004.
16. Taketomi Y, Sunaga K, Tanaka S, Nakamura M, Arata S, Okuda T, Moon TC, Chang HW, Sugimoto Y, Kokame K, Miyata T, Murakami M and Kudo I: Impaired mast cell maturation and degranulation and attenuated allergic responses in Ndrg1-deficient mice. J Immunol 178: 7042-7053, 2007.
17. Guan RJ, Ford HL, Fu Y, Li Y, Shaw LM and Pardee AB: Drg-1 as a differentiation-related, putative metastatic suppressor gene in human colon cancer. Cancer Res 60: 749-755, 2000.
18. Qu X, Zhai Y, Wei H, Zhang C, Xing G, Yu Y and He F: Characterization and expression of three novel differentiation-related genes belong to the human NDRG gene family. Mol Cell Biochem 229: 35-44, 2002.
19. Zhou RH, Kokame K, Tsukamoto Y, Yutani C, Kato H and Miyata T: Characterization of the human NDRG gene family: a newly identified member, NDRG4, is specifically expressed in brain and heart. Genomics 73: 86-97, 2001.
20. Lachat P, Shaw P, Gebhard S, van Belzen N, Chaubert P and Bosman FT: Expression of NDRG1, a differentiation-related gene, in human tissues. Histochem Cell Biol 118: 399-408, 2002.
21. Piquemal D, Joulia D, Balaguer P, Basset A, Marti J and Commes T: Differential expression of the RTP/Drg1/Ndr1 gene product in proliferating and growth arrested cells. Biochim Biophys Acta 1450: 364-373, 1999.
22. Bandyopadhyay S, Pai SK, Gross SC, Hirota S, Hosobe S, Miura K, Saito K, Commes T, Hayashi S, Watabe M and Watabe K: The Drg-1 gene suppresses tumor metastasis in prostate cancer. Cancer Res 63: 1731-1736, 2003.
23. Bandyopadhyay S, Pai SK, Hirota S, Hosobe S, Takano Y, Saito K, Piquemal D, Commes T, Watabe M, Gross SC, Wang Y, Ran S and Watabe K: Role of the putative tumor metastasis suppressor gene Drg-1 in breast cancer progression. Oncogene 23: 5675-5681, 2004.
24. Shah MA, Kemeny N, Hummer A, Drobnjak M, Motwani M, Cordon-Cardo C, Gonen M and Schwartz GK: Drg1 expression in 131 colorectal liver metastases: correlation with clinical variables and patient outcomes. Clin Cancer Res 11: 3296-3302, 2005.
25. Cangul H: Hypoxia upregulates the expression of the NDRG1 gene leading to its overexpression in various human cancers. BMC Genet 5: 27, 2004.
26. Wang Z, Wang F, Wang WQ, Gao Q, Wei WL, Yang Y and Wang GY: Correlation of N-myc downstream-regulated gene 1 overexpression with progressive growth of colorectal neoplasm. World J Gastroenterol 10: 550-554, 2004.
27. Chua MS, Sun H, Cheung ST, Mason V, Higgins J, Ross DT, Fan ST and So S: Overexpression of NDRG1 is an indicator of poor prognosis in hepatocellular carcinoma. Mod Pathol 20: 76-83, 2007.
28. Sibold S, Roh V, Keogh A, Studer P, Tiffon C, Angst E, Vorburger SA, Weimann R, Candinas D and Stroka D: Hypoxia increases cytoplasmic expression of NDRG1, but is insufficient for its membrane localization in human hepatocellular carcinoma. FEBS Lett 581: 989-994, 2007.
29. Hirohashi S, Ishak KG, Kojiro M, *et al*: World Health Organization Classification of Tumours. Pathology & Genetics of Tumours of Digestive System. Hepatocellular carcinoma. Hamilton SR and Aaltonen LA (eds). IARC Press, Lyon, pp159-172, 2000.
30. Nishie A, Masuda K, Otsubo M, Migita T, Tsuneyoshi M, Kohno K, Shuin T, Naito S, Ono M and Kuwano M: High expression of the Cap43 gene in infiltrating macrophages of human renal cell carcinomas. Clin Cancer Res 7: 2145-2151, 2001.
31. Maruyama Y, Ono M, Kawahara A, Yokoyama T, Basaki Y, Kage M, Aoyagi S, Kinoshita H and Kuwano M: Tumor growth suppression in pancreatic cancer by a putative metastasis suppressor gene Cap43/NDRG1/Drg-1 through modulation of angiogenesis. Cancer Res 66: 6233-6242, 2006.
32. Kutami R, Nakashima Y, Nakashima O, Shiota K and Kojiro M: Pathomorphologic study on the mechanism of fatty change in small hepatocellular carcinoma of humans. J Hepatol 33: 282-289, 2000.
33. Salnikow K, Blagosklonny MV, Ryan H, Johnson R and Costa M: Carcinogenic nickel induces genes involved with hypoxic stress. Cancer Res 60: 38-41, 2000.

Fucoidan, a major component of brown seaweed, prohibits the growth of human cancer cell lines *in vitro*

SUGURU FUKAHORI[1-3], HIROHISA YANO[1,3], JUN AKIBA[1,3], SACHIKO OGASAWARA[1,3], SEIYA MOMOSAKI[1,3], SAKIKO SANADA[1,3], KEITARO KURATOMI[1,3], YASUHIRO ISHIZAKI[1,3], FUKUKO MORIYA[1,3], MINORU YAGI[2,3] and MASAMICHI KOJIRO[1,3]

[1]Departments of Pathology, and [2]Pediatric Surgery, Kurume University School of Medicine; [3]Research Center of Innovative Cancer Therapy of the 21st Century COE Program for Medical Science, Kurume University, Kurume 830-0011, Japan

Received March 7, 2008; Accepted April 30, 2008

Abstract. Fucoidan, the general term for sulfated polysaccharides, is reported to engage in various biological activities having anti-tumor, anti-coagulation and anti-viral effects. Though it has been investigated, the mechanism of its anti-tumor effects remains elusive. The current study examined the anti-tumor effects of fucoidan extracted from Okinawa mozuku on 15 human cancer cell lines (6 hepatocellular carcinomas, 1 cholangiocarcinoma, 1 gallbladder cancer, 2 ovarian cancers, 1 hepatoblastoma, 1 neuroblastoma and 3 renal cancers) using an MTT assay. Changes in apoptosis and the cell cycle were analyzed by flow cytometry. The results revealed that cell proliferation was suppressed in 13 cell lines in a time- and/or dose-dependent manner; this suppression was marked in the hepatocellular carcinoma, cholangiocarcinoma and gallbladder carcinoma cell lines. In contrast, proliferation of the neuroblastoma and 1 of the 2 ovarian carcinoma cell lines was not affected. The ratio of apoptotic cells significantly increased in 5 of the 6 hepatocellular carcinoma cell lines, and the ratio of G_2/M cells increased in the 3 hepatocellular cell lines examined. These observations indicate that fucoidan is a potential anti-tumor agent for the treatment of bile duct cancers, such as hepatocellular carcinoma, cholangiocarcinoma and gall-bladder carcinoma.

Introduction

Malignant tumors are a major cause of death in humans and, though treatment methods for cancer have markedly progressed, curative regimens and protocols are still under investigation. At present, chemotherapy is regarded as the most effective treatment for solid tumors.

Correspondence to: Dr Suguru Fukahori, Department of Pathology and Pediatric Surgery, Kurume University School of Medicine, 67 Asahi-machi, Kurume, Fukuoka 830-0011, Japan
E-mail: s_fukahori@med.kurume-u.ac.jp

Key words: fucoidan, apoptosis, cell cycle, anti-tumor

Recent studies have shown that the natural substances extracted from green tea (1) and marine products, among others, have favorable preventive effects against cancers. 'Mozuku' (brown seaweed) is a marine plant which grows offshore around Okinawa Island. It has attracted the attention of scientists as well as the general public, and is considered a food which has various beneficial effects on the body. Fucoidan, the major component of 'mozuku', is the general term used for sulfated polysaccharides, which are also found in other seaweeds such as 'wakame', 'hijiki', 'mekabu'. Sulfated polysaccharides are reported to engage in various biological activities having anti-tumor effects (2-6), anti-thrombin activity (7,8), anti-coagulant activity (9) and anti-viral effects (10,11). Their anti-tumor effects have been investigated using various methods, but the mechanism of their action has remained elusive.

In order to increase the understanding of these anti-tumor effects, this *in vitro* study was conducted using 15 cell lines from 5 types of human cancers (liver cancer, cholangiocarcinoma, ovarian cancer, hepatoblastoma and neuroblastoma) along with fucoidan extracted from 'Okinawa mozuku'.

Materials and methods

Preparation of culture medium with fucoidan. Fucoidan solution was kindly provided by FCC Horiuchi & Co. (Kurume, Japan). The fucoidan was extracted from mozuku (*Cladosiphon Okamuranus Tokida*) collected from the shores of Okinawa Island in Japan, sold as a sea product (containing fucose 22.1 mg/100 mg) with government approval, and used as raw material for a health drink. The structure of the polysaccharide from *C. okamuranus* has been investigated previously (12,13).

The basal medium for cell culture was Dulbecco's modified Eagle's medium (Nissui Seiyaku Co., Tokyo, Japan) supplemented with 5% fetal bovine serum (Whittaker Bioproducts Inc., Walkersville, MD), 100 units/ml penicillin, and 100 μg/ml streptomycin (Gibco, Chagrin Falls, OH). Fucoidan was diluted with this medium and prepared in 10 concentrations (0.35, 0.70, 1.40, 2.82, 5.63, 11.25, 22.50, 45, 90 and 180 μg/ml). The osmotic pressures and pH values of the cultures with or without fucoidan were within normal physiological range.

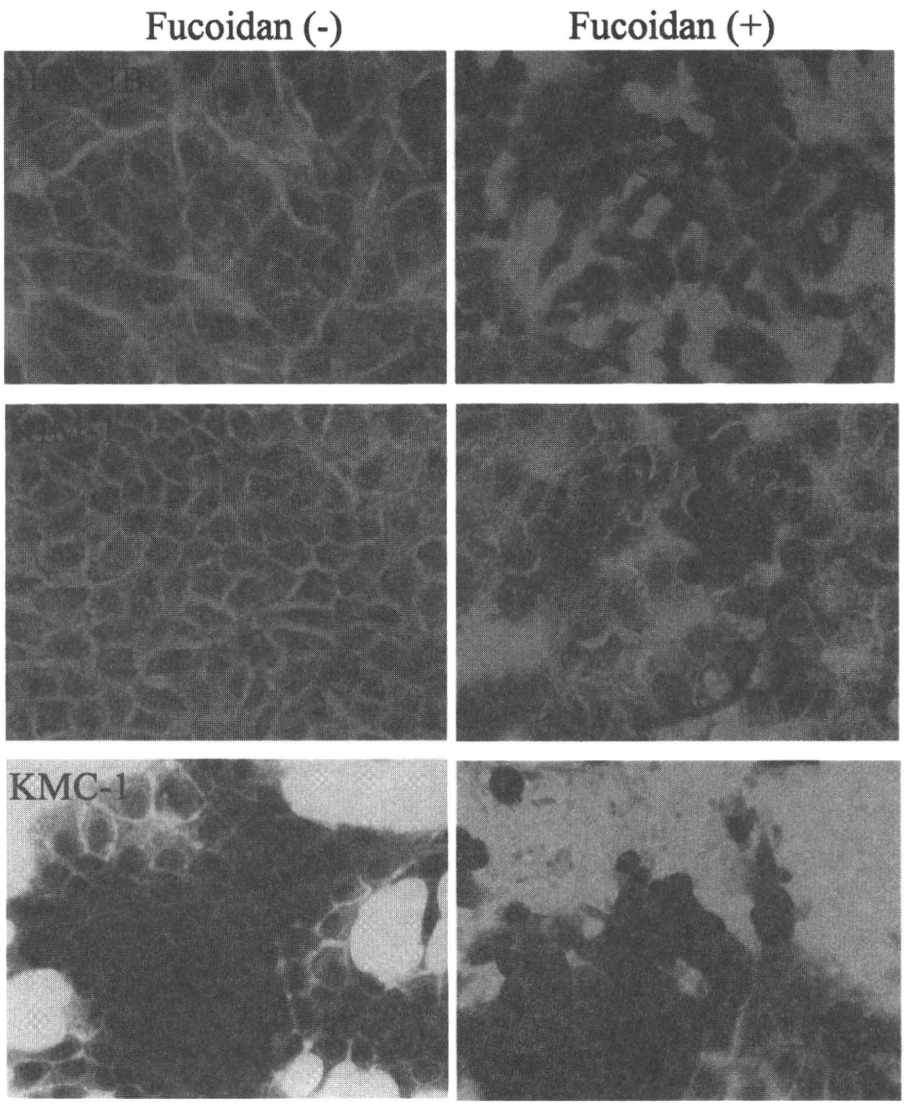

Figure 1. Photomicrograph of HAK-1B (A and B), KIM-1 (C and D) and KMC-1 (E and F) cells cultured for 72 h on a Lab-Tek Chamber slide. (A, C and E) No fucoidan in culture medium. Some mitotic figures were noted. (B, D and F) With 22.5 μg of fucoidan in culture medium. Apoptotic cells were characterized by cytoplasmic shrinkage, chromatic condensation and nuclear fragmentation (H&E staining, x200).

Cell lines and cell culture. Fifteen cell lines were used. These included 6 human hepatocellular carcinoma (HCC) cell lines [KIM-1 (12,14), KYN-1 (15), KYN-2 (16), KYN-3 (17), HAK-1A, HAK-1 (18)], one cholangiocarcinoma cell line (KMC-1) (19) and one gallbladder carcinoma cell line (KMG-C) which were originally established in our laboratory. Two human ovarian clear cell carcinoma cell lines (KOC-5C and KOC-7C) were established as described elsewhere (20,21), as were 3 human renal cell carcinoma cell lines (KURU II, KURM and OSRC2) (22). The human neuroblastoma cell line (SK-N-SE) was a generous gift from Dr K. Ueda of the Department of Pediatrics and Child Health of Kurume University. The human hepatoblastoma cell line (HuH-6) was purchased from the Japan Health Sciences Foundation (Osaka, Japan).

Observation of morphological changes. For light microscopic observations, the cells were seeded on Lab-Tek Tissue Culture Chamber Slides (Nunc Inc., Roskilde, Denmark), cultured with or without fucoidan (2.82, 22.5 or 90 μg/ml) for 72 h, fixed in Carnoy's solution for 10 min, then stained with hematoxylin and eosin (H&E) and observed under a microscope (Olympus BH-2, Olympus Optical, Tokyo, Japan).

Effect of fucoidan on the proliferation of each cell line. The effect of fucoidan on cell proliferation was investigated with colorimetric assays using MTT [3-(4,5-dimethylthiazol-2yl-yl)-2,5-diphenyltetrazolium bromide] cell growth assay kits (Chemicon International Inc., Temecula, CA) as previously described (23). Briefly, cells were seeded on 96-well plates (Falcon, Becton Dickinson Labware, Tokyo, Japan) and cultured for 24 h. The medium was then replaced with 100 μl of fresh medium alone or containing the diluted fucoidan solution (0.35, 0.70, 1.40, 2.82, 5.63, 11.25, 22.50, 45, 90 or 180 μg/ml). After 24, 48, 72 or 96 h, the number of viable cells was counted. Each experiment was repeated at least twice. The 50% inhibitory concentration (IC_{50}) was defined as the fucoidan concentration (μg) that caused a 50% reduction

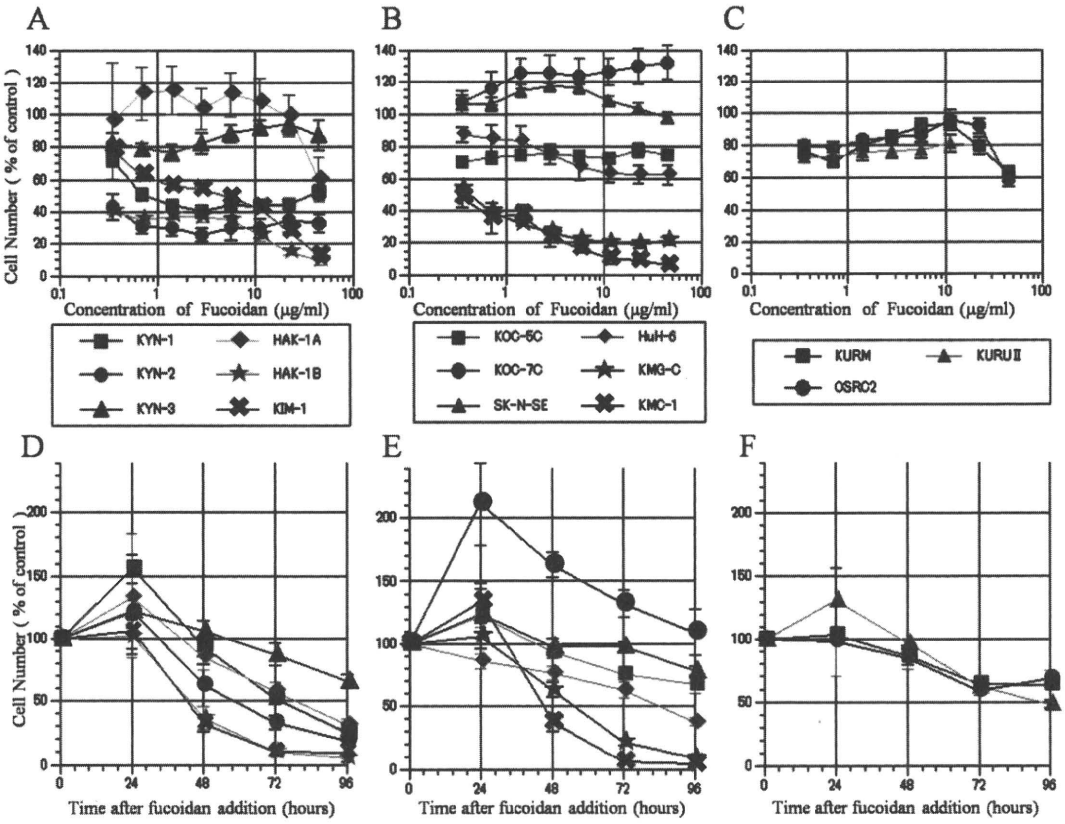

Figure 2. Antiproliferative effect of fucoidan (A-C) 72 h after 0.35, 0.70, 1.40, 2.82, 5.63, 11.25, 22.50 or 45 μg were added. Cell proliferation was suppressed in a dose-dependent manner in the 4 cell lines (KIM-1, HAK-1B, KMG-C, KMC-1), but not in the other 11 cell lines. The values represent the means ± SE of the experiments. The experiment was repeated at least twice for each cell line. (D-F) Chronological changes in the relative viable cell number (% of the control) after adding 22.5 μg of fucoidan. A time-dependent growth inhibition was observed in 13 cell lines with the exception of KOC-7C, and growth was suppressed over time to varying degrees.

in cellular viability. The IC_{50} value was calculated and used as a parameter in the comparison of the relative cytotoxicity of each cell line.

Quantitative analysis of fucoidan-induced apoptosis. Six HCC cell lines were cultured with or without fucoidan (22.5 or 90 μg/ml) for 72 h and then stained with Annexin V-EGFP (enhanced green fluorescent protein) using Apoptosis Detection Kits (Medical & Biological Laboratories, Nagoya, Japan) according to the manufacturer's protocol. After staining, the cells were analyzed using a FACScan (Becton Dickinson Immunocytometry Systems, San Jose, CA), and the percentage of Annexin V-EGFP-positive cells was determined.

Cell cycle analysis. Three HCC cell lines (HAK-1A, KYN-2, KYN-3) were cultured with or without fucoidan (22.5 μg/ml) for 24, 48 or 72 h, labeled with 10 μmol/l BrdUrd for 30 min, fixed in 70% cold ethanol at 4°C overnight, and stained with anti-BrdUrd antibody and propidium iodide (Sigma Chemical Co., St. Louis, MO) using a previously described technique (23). The stained cells were analyzed by FACScan using the CellQuest software program (ver. 3.3, Becton Dickinson). The distribution of cells in the G_0/G_1, S, or G_2/M phase of the cell cycle was calculated and shown as a percentage of each phase.
Statistical analysis. All data were expressed as the means ± SD. For data analysis, the Student's t-test was used. A P-value <0.05 was considered to be statistically significant.

Results

Effect of fucoidan on morphological changes. Cell morphology 72 h after the addition of fucoidan solution was observed using H&E staining. The cell density in culture decreased dose-dependently (except for neuroblastoma) in order from HCC (KIM-1, HAK-1A, HAK-1B, KYN-1, KYN-2, KYN-3), cholangiocarcinoma (KMC-1), gallbladder carcinoma (KMG-C), renal cell carcinoma (KURU II, KURM, OSRC2), to ovarian cancer (KOC-5C, KOC-7C). The cell density of the neuroblastoma cell line (SK-N-SE) did not decrease at any concentration of fucoidan. As shown in Fig. 1, 3 HCC cell lines (HAK-1B, KIM-1 and KMC-1) presented dose-dependent apoptotic changes such as nuclear condensation, cell shrinkage and nuclear fragmentation.

Effects of fucoidan on cell proliferation. MTT assay revealed chronological and dose-dependent suppression of the proliferation of 4 cell lines (HAK-1B, KIM-1, KMG-C and KMC-1), chronological suppression in 9 cell lines (KYN-1, KYN-2, KYN-3, HAK-1A, KOC-5C, HuH-6, KURM, OSRC2, KURU II), and no suppression in 2 cell lines (KOC-7C, SK-N-SE) (Fig. 2).

The IC_{50} values at 72 h of culture ranged from 18.71 to 299.20 μg/ml. Levels at 72 h could not be obtained for KMG-C, KMC-1, HAK-1B and KYN-2 because >50% suppression occurred; however, at 48 h the IC_{50} was 13.33 μg for

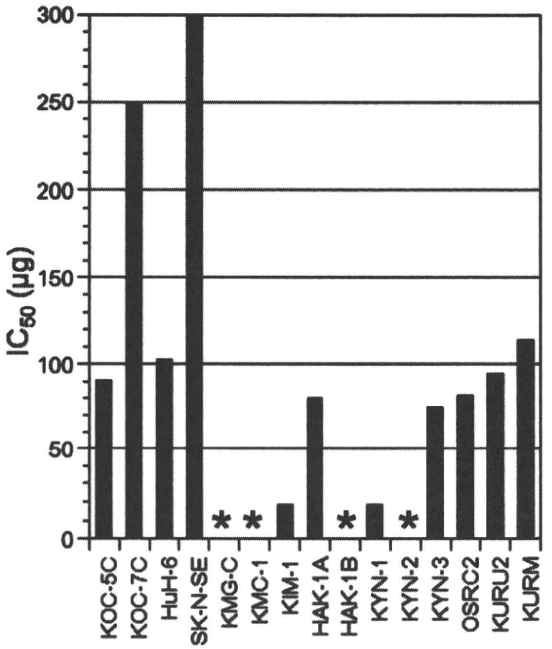

Figure 3. The IC_{50} of 15 cell lines treated with fucoidan for 72 h. *The IC_{50} values of KMG-C, KMC-1, HAK-1B and KYN-2 cell lines at 72 h could not be analyzed because the viable cell number was suppressed to <50% for all concentration levels of fucoidan.

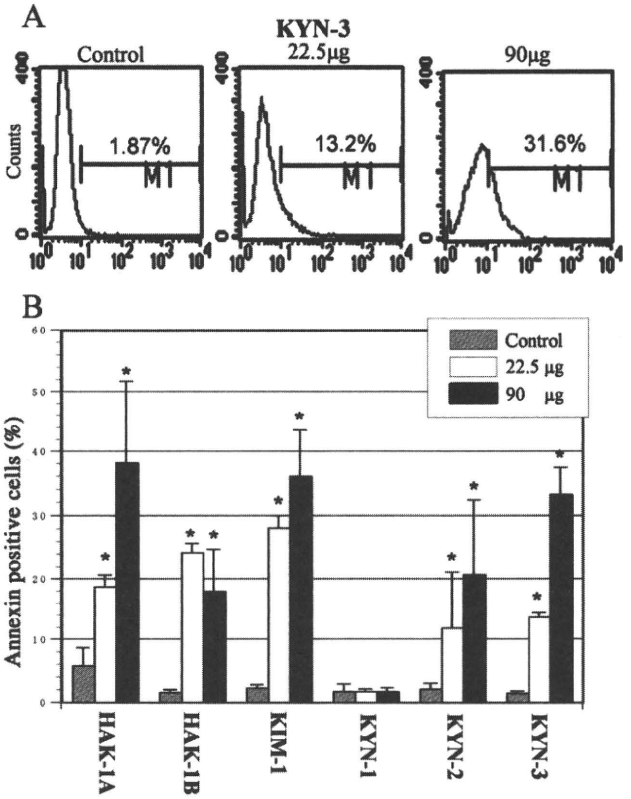

Figure 4. An analysis of apoptosis in 6 hepatocellular carcinoma cell lines treated with or without fucoidan for 72 h. HAK-1A, HAK-1B, KIM-1, KYN-1, KYN-2 and KYN-3 cell lines were treated with or without fucoidan (22.5 or 90 μg) for 72 h. The cells were harvested, labeled with Annexin-V-FITC and then analyzed by flow cytometry. (A) Percentage of apoptotic cells in the KYN-3 cell line. (B) Data represent the average (± SE) percentage of apoptotic cells. *P<0.001 vs. untreated cells.

KMC-1, 50.64 μg for HAK-1B, 52.32 μg for KYN-2 and 76.25 μg for KMG-C. According to tumor type, the IC_{50} was lowest in HCC and cholangiocarcinoma (Fig. 3).

Effect of fucoidan on apoptosis. Apoptosis was examined at 72 h of culture in the 6 cell lines that presented pronounced growth suppression in the MTT assay. The number of apoptotic cells increased significantly in the 5 HCC cell lines with the exception of KYN-1, indicating that fucoidan induced apoptosis (Fig. 4).

Effect of fucoidan on the cell cycle. Flow cytometry of the 3 HCC cell lines (HAK-1A, KYN-2, KYN-3) revealed an increased number of cells in the G_2/M phase at 72 h after the addition of the fucoidan solution (22.5 μg/ml) to the culture (Table I).

Discussion

The current study examined the anti-tumor effect of Okinawa mozuku fucoidan on 15 human cancer cell lines. Chronological and/or dose-dependent suppression of cell proliferation was observed in 13 of the 15 lines (87%). Previous studies have reported direct anti-tumor effects of fucoidan on HTLV-1-infected T cell lines and primary ATL cells (24), lymphoma cells (25) and a bronchopulmonary carcinoma cell line (NSCLC-N6) (4). The various possible mechanisms of fucoidan have also been explored, such as its anti-tumor effect induced by anti-angiogenesis (5), growth suppression due to immunopotentiation (26), and the suppression of metastasis (27,28), but only on one cell line. This current study investigated the effects had by fucoidan from the same source at the same time on multiple cell lines.

The major components of fucoidan are L-fucose and sulfate content. Previous studies used fucoidan extracted from *Fucus vesiculosus* (25), *Ascophyllum nodosum* (4,7), *Sargassum kjellmanianum* (29), *Sargassum thunbergii* (26) or *Cladosiphon okamuranus Tokida* (24), in which the percentage of L-fucose ranged from 12.6 to 36.0%, and the percentage of sulfate content from 8 to 25%. Sulfate content was also reported to be a factor with growth suppression effects (4,29). The fucoidan solution used in the current study contained these 2 substances within the above-mentioned ranges.

In this study, the suppression of cell proliferation was more apparent in the cell lines of HCC, cholangiocarcinoma and gallbladder carcinoma than in those of neuroblastoma, hepatoblastoma, ovarian carcinoma and renal carcinoma. The growth suppression effects also varied among the cell lines of the same tumor type. The IC_{50} values of the HAK-1B (HCC) and KMC-1 (cholangiocarcinoma) cell lines were additionally markedly lower in comparison to previously reported data (4,25). These findings indicate that the anti-tumor effects of fucoidan vary according to tumor type and, along with previous findings, demonstrate the anti-tumor effects of fucoidan on colon cancer but not on mammary tumors (30). This indicates that the supression of cell proliferation does not occur in all cancer cell lines. The mechanism behind the more potent growth suppression observed in the HCC and cholangiocarcinoma cell lines should therefore be explored in future studies.

Table I. Flow cytometric analysis of the effect of fucoidan (22.5 μg/ml) on the cell cycle of hepatocellular carcinoma cell lines at 24, 48 and 72 h of culture.

		24 h		48 h		72 h	
Cell line	Cell cycle	Control	Fucoidan	Control	Fucoidan	Control	Fucoidan
HAK-1A	G_0/G_1	30.7	24.3	38.4	22.8	42.9	20.5
	S	48.8	37.6	36.9	46.3	38.1	44.1
	G_2/M	16.2	22.9	18.9	22.4	13.9	19.2
KYN-2	G_0/G_1	26.1	28.8	31.9	32.2	34.0	44.4
	S	57.7	31.2	46.8	37.7	32.1	21.1
	G_2/M	12.2	28.6	9.7	20.1	18.6	23.5
	G_0/G_1	32.0	35.2	42.1	37.8	46.0	49.4
KYN-3	S	53.6	27.0	41.4	34.8	35.7	29.5
	G_2/M	9.5	31.9	11.1	23.5	12.9	17.0

Control, cells cultured without fucoidan. Fucoidan, cells cultured with fucoidan (22.5 μg/ml). Values represent the percentage of cells at each phase of the cell cycle.

Haneji *et al* (24) reported that apoptosis is induced by the activation of the caspase pathway, and Aisa *et al* (25) demonstrated anti-tumor effects accompanied by the activation of the caspase pathway and the down-regulation of the ERK pathway. In the current study, 5 of the 6 HCC cell lines presented a significant dose-dependent increase in apoptosis. The activation of caspase-3 and -9 in HAK-1B, which presented marked apoptosis, was therefore investigated. However, no clear activation was observed (data not shown), indicating that the anti-tumor effects of fucoidan on HCC cell lines could be associated with a different pathway.

With regard to cell cycle effect, Haneji *et al* (24) reported that fucoidan induced the accumulation of cells in the G_1/S phase, and Riou *et al* (4) observed that anti-tumor effects were accompanied by a G_1 phase block. On the other hand, Aisa *et al* (25) reported no effect on the cell cycle. The current findings regarding the cell cycle demonstrate for the first time an increase in cells in the G_2/M phase.

In the current study, fucoidan suppressed cell proliferation in a time- and dose-dependent manner at various degrees, and its effects were particularly pronounced in the HCC, cholangiocarcinoma and gallbladder carcinoma cell lines. The results indicate that the mechanisms of fucoidan action include the induction of apoptosis and the inhibition of the cell cycle.

At present, the clinical results of treatment for advanced HCC and cholangiocarcinoma are unsatisfactory. Fucoidan could be a potential anti-tumor remedy for specific cancers, such as HCC or cholangiocarcinoma. More detailed information on the anti-tumor effects of fucoidan should therefore be obtained in future animal studies.

Acknowledgements

We thank Ms. Akemi Fujiyoshi for her valuable assistance with our experiments.

References

1. Nakachi K, Matsuyama S, Miyake S, Suganuma M and Imai K: Preventive effects of drinking green tea on cancer and cardiovascular disease: epidemiological evidence for multiple targeting prevention. Biofactors 13: 49-54, 2000.
2. Parish CR, Coombe DR, Jakobsen KB, Bennett FA and Underwood PA: Evidence that sulfated polysaccharides inhibit tumour metastasis by blocking tumour-cell-derived heparanases. Int J Cancer 40: 511-518, 1987.
3. Zhuang C, Itoh H, Mizuno T and Ito H: Antitumor active fucoidan from the brown seaweed, umitoranoo (Sargassum thunbergii). Biosci Biotechnol Biochem 59: 563-567, 1995.
4. Riou D, Colliec-Jouault S, Pinczon du Sel D, *et al*: Antitumor and antiproliferative effects of a fucan extracted from ascophyllum nodosum against a non-small-cell broncho-pulmonary carcinoma line. Anticancer Res 16: 1213-1218, 1996.
5. Koyanagi S, Tanigawa N, Nakagawa H, Soeda S and Shimeno H: Oversulfation of fucoidan enhances its anti-angiogenic and antitumor activities. Biochem Pharmacol 65: 173-179, 2003.
6. Maruyama H, Tamauchi H, Hashimoto M and Nakano T: Antitumor activity and immune response of Mekabu fucoidan extracted from Sporophyll of Undaria pinnatifida. In Vivo 17: 245-249, 2003.
7. Colliec S, Fischer AM, Tapon-Bretaudiere J, Boisson C, Durand P and Jozefonvicz J: Anticoagulant properties of a fucoidan fraction. Thromb Res 64: 143-154, 1991.
8. Trento F, Cattaneo F, Pescador R, Porta R and Ferro L: Antithrombin activity of an algal polysaccharide. Thromb Res 102: 457-465, 2001.
9. Durig J, Bruhn T, Zurborn KH, Gutensohn K, Bruhn HD, and Beress L: Anticoagulant fucoidan fractions from Fucus vesiculosus induce platelet activation in vitro. Thromb Res 85: 479-491, 1997.
10. Baba M, Schols D, Pauwels R, Nakashima H and De Clercq E: Sulfated polysaccharides as potent inhibitors of HIV-induced syncytium formation: a new strategy towards AIDS chemotherapy. J Acquir Immune Defic Syndr 3: 493-499, 1990.
11. McClure MO, Moore JP, Blanc DF, *et al*: Investigations into the mechanism by which sulfated polysaccharides inhibit HIV infection in vitro. AIDS Res Hum Retroviruses 8: 19-26, 1992.
12. Nagaoka M, Shibata H, Kimura-Takagi I, *et al*: Structural study of fucoidan from Cladosiphon okamuranus tokida. Glycoconj J 16: 19-26, 1999.
13. Sakai T, Ishizuka K, Shimanaka K, Ikai K and Kato I: Structures of oligosaccharides derived from *Cladosiphon okamuranus* fucoidan by digestion with marine bacterial enzymes. Mar Biotechnol 5: 536-544, 2003.

14. Murakami T: Establishment and characterization of a new human hepatocellular carcinoma cell line (KIM-1). Acta Hepatol Jpn 25: 532-539, 1988.
15. Yano H, Kojiro M and Nakashima T: A new human hepatocellular carcinoma cell line (KYN-1) with a transformation to adenocarcinoma. In Vitro Cell Dev Biol 22: 637-646, 1986.
16. Yano H, Maruiwa M, Murakami T, *et al*: A new human pleomorphic hepatocellular carcinoma cell line, KYN-2. Acta Pathol Jpn 38: 953-966, 1988.
17. Murakami T, Maruiwa M, Fukuda K, Kojiro M, Tanaka M and Tanikawa K: Characterization of a new human hepatoma cell line (KYN-3) derived from the ascites of the hepatoma patient [abstract]. Jpn J Cancer Res Proceedings of the Japanese Cancer Association 192, 1988.
18. Yano H, Iemura A, Fukuda K, Mizoguchi A, Haramaki M and Kojiro M: Establishment of two distinct human hepatocellular carcinoma cell lines from a single nodule showing clonal dedifferentiation of cancer cells. Hepatology 18: 320-327, 1993.
19. Iemura A, Maruiwa M, Yano H and Kojiro M: A new human cholangiocellular carcinoma cell line (KMC-1). J Hepatol 15: 288-298, 1992.
20. Tomioka Y: Establishment and characterization of three human ovarian clear cell carcinoma cell line. J Kurume Med Assoc 61: 323-333, 1998.
21. Takemoto Y, Yano H, Momosaki S, *et al*: Antiproliferative effects of interferon-alphaCon1 on ovarian clear cell adenocarcinoma *in vitro* and *in vivo*. Clin Cancer Res 10: 7418-7426, 2004.
22. Inoue M, Yano H and Kojiro M: Expression of Fas and anti-mediated apoptosis in human renal cell carcinoma. Int J Oncol 9: 49-56, 1996.
23. Yano H, Iemura A, Haramaki M, *et al*: Interferon alfa receptor expression and growth inhibition by interferon alfa in human liver cancer cell lines. Hepatology 29: 1708-1717, 1999.
24. Haneji K, Matsuda T, Tomita M, *et al*: Fucoidan extracted from Cladosiphon okamuranus Tokida induces apoptosis of human T cell leukemia virus type 1-infected T-cell lines and primary adult T-cell leukemia cells. Nutr Cancer 52: 189-201, 2005.
25. Aisa Y, Miyakawa Y, Nakazato T, *et al*: Fucoidan induces apoptosis of human HS-sultan cells accompanied by activation of caspase-3 and down-regulation of ERK pathways. Am J Hematol 78: 7-14, 2005.
26. Itoh H, Noda H, Amano H and Ito H: Immunological analysis of inhibition of lung metastases by fucoidan (GIV-A) prepared from brown seaweed Sargassum thunbergii. Anticancer Res 15: 1937-1947, 1995.
27. Coombe DR, Parish CR, Ramshaw IA and Snowden JM: Analysis of the inhibition of tumour metastasis by sulphated polysaccharides. Int J Cancer 39: 82-88, 1987.
28. Liu JM, Haroun-Bouhedja F and Boisson-Vidal C: Analysis of the in vitro inhibition of mammary adenocarcinoma cell adhesion by sulphated polysaccharides. Anticancer Res 20: 3265-3271, 2000.
29. Yamamoto I, Takahashi M, Suzuki T, Seino H and Mori H: Antitumor effect of seaweeds. IV. Enhancement of antitumor activity by sulfation of a crude fucoidan fraction from Sargassum kjellmanianum. Jpn J Exp Med 54: 143-151, 1984.
30. Ellouali M, Boisson-Vidal C, Durand P and Jozefonvicz J: Antitumor activity of low molecular weight fucans extracted from brown seaweed Ascophyllum nodosum. Anticancer Res 13: 2011-2019, 1993.